

**OPEN ACCESS****EDITED BY**

Nicolao Fornengo,
University of Turin, Italy

REVIEWED BY

Mattia Di Mauro,
National Institute of Nuclear Physics of
Turin, Italy
Antonio Martin-Carrillo,
University College Dublin, Ireland

***CORRESPONDENCE**

Javier A. García,
✉ javier.a.garciamartinez@nasa.gov

[†]NASA Hubble Fellowship Program (NFHP)
Einstein Fellow

RECEIVED 27 July 2024

ACCEPTED 07 October 2024

PUBLISHED 25 November 2024

CITATION

García JA, Stern D, Madsen K, Smith M, Grefenstette B, Ajello M, Alford J, Annuar A, Bachetti M, Baloković M, Beckmann RS, Bianchi S, Biccaro D, Boorman P, Brightman M, Buchner J, Bulbul E, Chen C-T, Civano F, Coley J, Connors RMT, Del Santo M, Gesu LD, Draghis PA, Fragile PC, Gúrpide A, Gangi M, Gezari S, Harrison F, Kammoun E, Lanzuisi G, Lehmer B, Lohfink A, Ludlam R, Marchesi S, Marcotulli L, Margutti R, Masterson M, Merloni A, Middleton M, Mori K, Moretti A, Nandra K, Perez K, Pfeifle RW, Pinto C, Piotrowska J, Ponti G, Pottschmidt K, Predehl P, Puccetti S, Rau A, Reynolds S, Santangelo A, Spiga D, Tomsick JA, Torres-Albà N, Walton DJ, Wilkins D, Wilms J, Zhang W and Zhao X (2024) The high energy X-ray probe (HEX-P): science overview. *Front. Astron. Space Sci.* 11:1471585. doi: 10.3389/fspas.2024.1471585

The high energy X-ray probe (HEX-P): science overview

Javier A. García^{1,2*}, Daniel Stern³, Kristin Madsen¹, Miles Smith³, Brian Grefenstette², Marco Ajello⁴, Jason Alford⁵, Adlyka Annuar⁶, Matteo Bachetti⁷, Mislav Baloković^{8,9}, Ricarda S. Beckmann¹⁰, Stefano Bianchi¹¹, Daniela Biccaro³, Peter Boorman², Murray Brightman², Johannes Buchner¹², Esra Bulbul¹², Chien-Ting Chen^{13,14}, Francesca Civano¹, Joel Coley^{1,15,16}, Riley M. T. Connors¹⁷, Melania Del Santo¹⁸, Laura Di Gesu¹⁹, Paul A. Draghis^{20,21}, P. Chris Fragile²², Andrés Gúrpide²³, Manuele Gangi¹⁹, Suvi Gezari²⁴, Fiona Harrison², Elias Kammoun^{11,25,26}, Giorgio Lanzuisi²⁷, Bret Lehmer²⁸, Anne Lohfink²⁹, Renee Ludlam³⁰, Stefano Marchesi^{4,27}, Lea Marcotulli^{8,9†}, Raffaella Margutti³¹, Megan Masterson²⁰, Andrea Merloni¹², Matthew Middleton²³, Kaya Mori³², Alberto Moretti³³, Kirpal Nandra¹², Kerstin Perez³², Ryan W. Pfeifle^{1,34}, Ciro Pinto¹⁸, Joanna Piotrowska², Gabriele Ponti³³, Katja Pottschmidt^{16,35}, Peter Predehl¹², Simonetta Puccetti¹⁹, Arne Rau¹², Stephen Reynolds³⁶, Andrea Santangelo³⁷, Daniele Spiga³³, John A. Tomsick³¹, Núria Torres-Albà⁴, Dominic J. Walton³⁸, Daniel Wilkins³⁹, Joern Wilms⁴⁰, Will Zhang¹ and Xiurui Zhao^{41,42}, on behalf of the HEX-P Collaboration

¹X-Ray Astrophysics Laboratory, National Aeronautics and Space Administration (NASA) Goddard Space Flight Center, Greenbelt, MD, United States, ²Cahill Center for Astronomy and Astrophysics, California Institute of Technology, Pasadena, CA, United States, ³Jet Propulsion Laboratory, California Institute of Technology, Pasadena, CA, United States, ⁴Department of Physics and Astronomy, Kinard Lab of Physics, Clemson University, Clemson, SC, United States, ⁵Department of Physics, New York University, Abu Dhabi, United Arab Emirates, ⁶Department of Applied Physics, Faculty of Science and Technology, Universiti Kebangsaan Malaysia, Selangor, Malaysia, ⁷Istituto Nazionale di Astrofisica (INAF)-Osservatorio Astronomico di Cagliari, Selargius, Italy, ⁸Department of Astronomy, Yale Center for Astronomy and Astrophysics, New Haven, CT, United States, ⁹Department of Physics, Yale University, New Haven, CT, United States, ¹⁰Institute of Astronomy and Kavli Institute for Cosmology, University of Cambridge, Cambridge, United Kingdom, ¹¹Dipartimento di Matematica e Fisica, Università degli Studi Roma Tre, Rome, Italy, ¹²Max-Planck-Institute for Extraterrestrial Physics, Garching, Germany, ¹³Science and Technology Institute, Universities Space Research Association, Huntsville, AL, United States, ¹⁴Astrophysics Office, National Aeronautics and Space Administration (NASA) Marshall Space Flight Center, Huntsville, AL, United States, ¹⁵Department of Physics and Astronomy, Howard University, Washington, DC, United States, ¹⁶Center for Research and Exploration in Space Science and Technology (CREST) and Center for Space Sciences and Technology (CSST), University of Maryland, Baltimore County, Baltimore, MD, United States, ¹⁷Department of Physics, Villanova University, Villanova, PA, United States, ¹⁸Istituto Nazionale di Astrofisica (INAF)/Istituto di Astrofisica Spaziale e Fisica (IASF) Palermo, Palermo, Italy, ¹⁹ASI - Agenzia Spaziale Italiana, Rome, Italy, ²⁰MIT Kavli Institute for Astrophysics and Space Research, Massachusetts Institute of Technology, Cambridge, MA, United States, ²¹Department of Astronomy, University of Michigan, Ann Arbor, MI, United States, ²²Department of Physics and Astronomy, College of Charleston, Charleston, SC, United States, ²³School of Physics and Astronomy, University of Southampton, Southampton, United Kingdom, ²⁴Space Telescope Science Institute, Baltimore, MD, United States, ²⁵Institut de Recherche en Astrophysique et Planétologie (IRAP), Université de Toulouse, Centre national de la recherche scientifique (CNRS), Université Paul Sabatier (UPS), Centre National d'études Spatiales (CNES), Toulouse, France, ²⁶Istituto Nazionale di Astrofisica (INAF) – Osservatorio Astrofisico di Arcetri, Florence, Italy

Firenze, Italy,²⁷Istituto Nazionale di Astrofisica (INAF) – Osservatorio di Astrofisica e Scienza dello Spazio, Bologna, Italy,²⁸Department of Physics, University of Arkansas, Fayetteville, AR, United States,²⁹Department of Physics, Montana State University, Bozeman, MT, United States,³⁰Department of Physics and Astronomy, Wayne State University, Detroit, MI, United States,³¹Space Sciences Laboratory, University of California, Berkeley, Berkeley, CA, United States,³²Columbia Astrophysics Laboratory, Columbia University, New York, NY, United States,³³Istituto Nazionale di Astrofisica (INAF)/Osservatorio Astronomico di Brera, Merate, LC, Italy,³⁴Oak Ridge Associated Universities, National Aeronautics and Space Administration (NASA) NASA Postdoctoral Program (NPP) Program, Oak Ridge, TN, United States,³⁵Astroparticle Physics Laboratory, National Aeronautics and Space Administration (NASA) Goddard Space Flight Center, Greenbelt, MD, United States,³⁶Department of Physics, North Carolina State University, Raleigh, NC, United States,³⁷Institute of Astronomy and Astrophysics, University of Tübingen, Tübingen, Germany,³⁸Centre for Astrophysics Research, University of Hertfordshire, Hatfield, United Kingdom,³⁹Kavli Institute for Particle Astrophysics and Cosmology, Stanford University, Stanford, CA, United States,⁴⁰Erlangen Centre for Astroparticle Physics and Remeis-Observatory, Friedrich-Alexander-Universität Erlangen-Nürnberg, Bamberg, Germany,⁴¹Department of Astronomy, University of Illinois at Urbana-Champaign, Urbana, IL, United States,⁴²Center for Astrophysics | Harvard and Smithsonian, Cambridge, MA, United States

To answer NASA's call for a sensitive X-ray observatory in the 2030s, we present the High Energy X-ray Probe (HEX-P) mission concept. HEX-P is designed to provide the required capabilities to explore current scientific questions and make new discoveries with a broadband X-ray observatory that simultaneously measures sources from 0.2 to 80 keV. HEX-P's main scientific goals include: 1) understand the growth of supermassive black holes and how they drive galaxy evolution; 2) explore the lower mass populations of white dwarfs, neutron stars, and stellar-mass black holes in the nearby universe; 3) explain the physics of the mysterious corona, the luminous plasma close to the central engine of accreting compact objects that dominates cosmic X-ray emission; and 4) find the sources of the highest energy particles in the Galaxy. These goals motivate a sensitive, broadband X-ray observatory with imaging, spectroscopic, and timing capabilities, ensuring a versatile platform to serve a broad General Observer (GO) and Guest Investigator (GI) community. In this paper, we present an overview of these mission goals, which have been extensively discussed in a collection of more than a dozen papers that are part of this Research Topic volume. The proposed investigations will address key questions in all three science themes highlighted by Astro2020, including their associated priority areas. HEX-P will extend the capabilities of the most sensitive low- and high-energy X-ray satellites currently in orbit and will complement existing and planned high-energy, time-domain, and multi-messenger facilities in the next decade.

KEYWORDS

x-ray, HEX-P, mission science, NASA, black holes, supernova, AGN, neutron stars - general

1 Introduction

Across the Universe there are mysteries whose secrets are encoded over three orders of magnitude in X-ray energy and more than nine orders in time. As black holes and neutron stars tear apart companions, the accreting matter shines brightly in X-rays from 0.1 to 100 keV. Broad spectral features tell the story of the interacting system and how it formed. Elsewhere in our Universe, extreme events are occurring as stars explode into their recent ejecta, merging neutron stars create ripples in the cosmic fabric, and stars are shredded as they plunge into black holes. And behind it all, billions of active galactic nuclei (AGN) sum together to produce the cosmic X-ray background that peaks at 25 keV. When resolved into individual sources, their spectra tell the story of whether each AGN is enshrouded in dust and gas, how fast its supermassive

central black hole is spinning, and whether it is producing feedback from a powerful outflow. These phenomena vary on timescales of milliseconds to millennia, and decoding their secrets requires simultaneous broadband observations.

At the center of all active galaxies exists a supermassive black hole ($10^6 - 10^{10} M_\odot$; SMBH), which is believed to play a crucial role in the evolution of its host galaxy. Accretion onto the SMBH is an efficient process to convert matter into energy, producing powerful radiation that outshines all the stars in the galaxy at high energies and drives a strong wind that both induces and inhibits star formation, shaping the very appearance of the galaxy. Light from a surrounding accretion disk is scattered to X-ray energies by a mysterious plasma, and those X-rays are also seen in reflection off the relativistic disk. The surrounding material is mostly opaque to

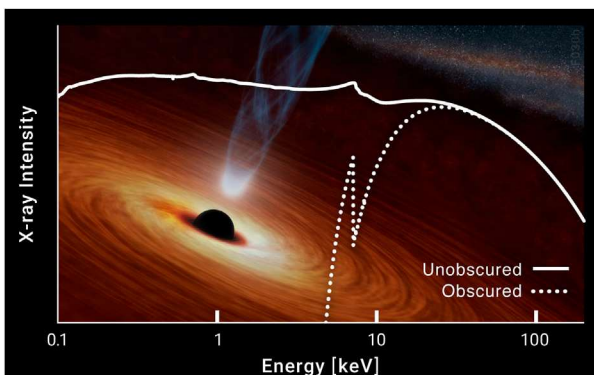


FIGURE 1
The primary emission from accretion is broadband. While accreting sources emit across the full 0.1–100 keV X-ray band, gas preferentially absorbs at low energy, making obscured sources best studied above 10 keV.

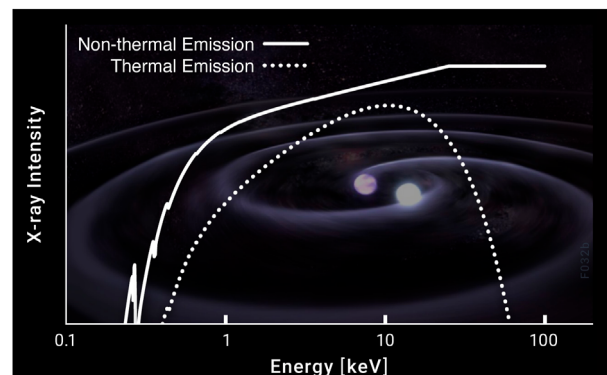


FIGURE 3
The primary emission from accretion is broadband. The X-ray band encodes key spectral features that reveal the physics underlying transient and multi-messenger events, such as sources of gravitational waves.

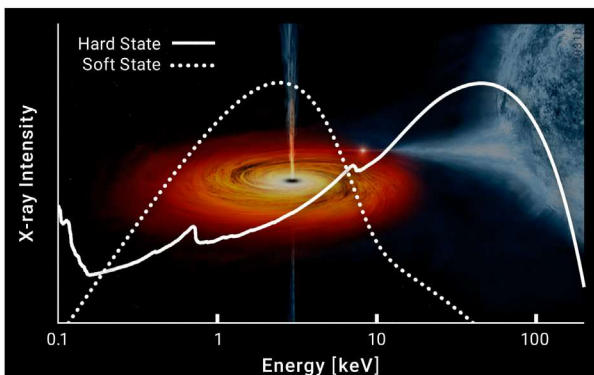


FIGURE 2
The primary emission from accretion is broadband. Accreting binary systems shift between hard and soft states, as emission from the corona (hard) or accretion disk (soft) dominate their energetics.

low-energy radiation, including soft X-rays, but hard X-ray photons ($\gtrsim 10$ keV) can easily penetrate and escape (Figure 1).

Meanwhile, stellar-mass black holes ($\sim 5 - 100 M_{\odot}$), which are formed via stellar gravitational collapse, are typically detected in X-rays when in binary systems. Luckily, massive stars are rarely born alone. They form in binaries and multiple systems, exchanging mass as they evolve. The stars' fates become intertwined as their very appearance and lifetimes are influenced by close companions. At late stages, after the more massive star has exploded, close binaries are revealed as the neutron star or black hole remnant violently absorbs matter from its companion. The strong accretion of matter transforms the system into a bright X-ray source, that switches from predominantly soft (< 10 keV) to hard (> 10 keV) states and back again as different physical processes dominate the emission mechanism (Figure 2).

In addition to the extreme environments created by active black holes, our Universe is adorned with a rich tapestry of explosive and

energetic events, producing X-rays as jets form, matter collides, and accreting systems are created or destroyed. Our Galaxy contains sites where magnetic fields accelerate ions and electrons to extreme energies, producing high-energy photons as they gyrate in the strong fields and collide with surrounding material. The high-energy spectra of these time-domain and multi-messenger events reveal the nature and physics of the source (Figure 3).

All these exciting astrophysical phenomena require an agile and versatile platform capable of producing simultaneous imaging, spectroscopy, and timing data across the entire X-ray band. The High-Energy X-ray Probe (HEX-P) mission was designed with these requirements in mind. HEX-P is a probe-class mission concept, as directed by the 2020 Decadal Survey on Astronomy and Astrophysics,¹ and was submitted in response to the 2023 NASA Astrophysics Probe Explorer (APEX) call. The observatory combines the power of high angular resolution with broad passband coverage to provide the necessary leap in capabilities to address the important astrophysical questions of the next decade. These were formulated in the Astro2020 Decadal Survey in the Cosmic Ecosystems context as unveiling the “Drivers of Galaxy Growth”: *to revolutionize our understanding of the origins and evolution of galaxies, for which new observational capabilities across the electromagnetic spectrum are needed to resolve the rich workings of galaxies on all scales.* HEX-P fills in the important gap between soft X-rays and γ -rays where compact objects, from stellar remnants (neutron stars and black holes) up to supermassive black holes, emit vast amounts of energy through the process of accretion. Powerful ionizing winds from such objects are believed to have a major impact on galaxy evolution, but the growth, numbers, and distribution of these compact objects are poorly understood and only accessible for our closest galactic neighbors.

The current X-ray mission landscape is dominated by oversubscribed observatories far into their extended operation

¹ <https://www.nationalacademies.org/our-work/decadal-survey-on-astronomy-and-astrophysics-2020-astro2020>

phase. The next planned flagship-class X-ray observatory is ESA's NewAthena mission, which is currently scheduled to launch no earlier than 2037. With this current outlook, the science community faces a non-negligible risk of being without a sensitive General Observer (GO) X-ray capability in the 2030s, just at the time that such an observatory is essential to inform the discoveries by the multiple time-domain and multi-messenger facilities coming online in the next decade. HEX-P is designed to bridge this gap with instrumentation that will deliver capabilities to advance our understanding of the X-ray Universe. HEX-P will peer into the hidden regions of the cosmos to reveal the most extreme astrophysical sources and events.

In this paper we present an overview of the core science that drives the HEX-P concept. This is the result of a several-months long study primarily led by members of the high-energy astrophysics community, in a voluntary manner, to determine the most compelling scientific objectives that can be addressed with a mission like HEX-P. A companion paper describing the mission design and implementation is presented by [Madsen et al. \(2024\)](#). More than 200 scientists have produced over a dozen peer-reviewed publications describing a comprehensive yet non-exhaustive list of science uniquely enabled by HEX-P, including topics such as accretion onto supermassive black holes, the cosmic X-ray background, the strong magnetic fields of neutron stars, and resolved studies of X-ray emission in supernova remnants, to name a few. These papers constitute the HEX-P Research Topic published by *Frontiers in Astronomy and Space Sciences*, which can be accessed freely at their online portal.²

2 Observatory and mission overview

The NASA Explorer Nuclear Spectroscopic Telescope Array (NuSTAR) ([Harrison et al., 2013](#)) opened the high-energy X-ray band by establishing the power of broad-band X-ray spectroscopy (3–80 keV). HEX-P builds on this legacy by expanding the low-energy passband down to 0.2 keV where thermal processes dominate, and by improving the angular resolution with different mirror technologies optimized over the passband. The observatory has a 20-meter focal length and the 0.2–80 keV passband is covered by the two instruments, the Low Energy Telescope (LET) and the High Energy Telescope (HET), which are co-aligned and observe the same field. The LET consists of the Low Energy Mirror Assembly (LEMA) and a Low Energy Detector Assembly (LEDA), and the HET of two High Energy Mirror Assemblies (HEMAs) matched to two High Energy Detector Assemblies (HEDAs). HEX-P will be launched into L1, which provides a high observing efficiency ($\geq 90\%$), which combined with a large field of regard allows for long and uninterrupted exposures. See [Madsen et al. \(2024\)](#) for details on the mission design, instrumentation and implementation. A short summary is provided below.

The LET consists of a segmented mirror assembly coated with Ir on monocrystalline silicon that achieves a half-power diameter

(HPD) of $3.5''$, and a low-energy DEPFET detector, of the same type as the Wide Field Imager (WFI; [Meidinger et al., 2020](#)) onboard NewAthena ([Nandra et al., 2013](#)). It has 512×512 pixels that cover a field of view of $11.3' \times 11.3'$. It has an effective passband of 0.2–25 keV, and a full frame readout time of 2 ms, which can be operated in a 128 or 64 channel window mode for higher count-rates to mitigate pile-up and faster readout. Pile-up effects remain below an acceptable limit of $\sim 1\%$ for a flux up to ~ 100 mCrab (2–10 keV) in the smallest window configuration. Excising the core of the PSF, a common practice in X-ray astronomy, will allow for observations of brighter sources, with a typical loss of up to $\sim 60\%$ of the total photon counts.

The HET consists of two co-aligned telescopes and detector modules. The optics are made of Ni-electroformed full shell mirror substrates, leveraging the heritage of XMM-Newton ([Jansen et al., 2001](#)), and coated with Pt/C and W/Si multilayers for an effective passband of 2–80 keV. The high-energy detectors are of the same type as flown on NuSTAR ([Harrison et al., 2013](#)), and they consist of 16 CZT sensors per focal plane, tiled 4×4 , for a total of 128×128 pixels spanning a field of view slightly larger than for the LET, $13.4' \times 13.4'$.

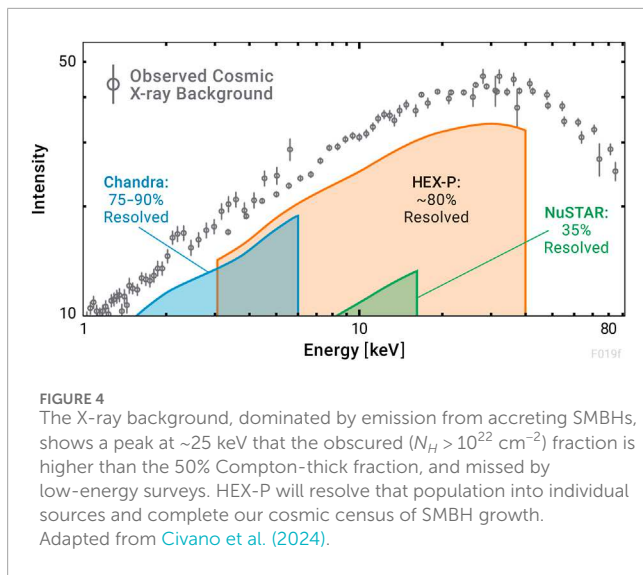
All the simulations presented in the collection of HEX-P papers discussed here were produced with a set of response files that represent the observatory performance based on current best estimates as of Spring 2023 (see [Madsen et al., 2024](#)). The effective area is derived from ray-tracing calculations for the mirror design including obscuration by all known structures. The detector responses are based on simulations performed by the respective hardware groups, with an optical blocking filter for the LET and a Be window and thermal insulation for the HET. The LET background was derived from a GEANT4 simulation ([Eraerds et al., 2021](#)) of the WFI instrument, and the HET backgrounds were derived from a GEANT4 simulation of the NuSTAR instrument. Both simulations adopt the L1 orbit for HEX-P.

The baseline mission is 5 years, with 30% of the observing time dedicated to the Principal Investigator (PI) led program and 70% to a GO program. The GO program will be executed alongside the PI-led, and data will be made available immediately with no proprietary time. With a large propellant capacity and strategic redundancies, HEX-P is designed to operate for more than 20 years.

3 Science enabled by HEX-P

In this Section we summarize the core scientific goals that will be addressed by the HEX-P mission. HEX-P seeks to answer fundamental questions highlighted by the Astro2020 Decadal Survey, delivering transformative science for compact objects and time-domain, multi-messenger astrophysics. The design of HEX-P's capabilities aims to address three main scientific goals to unravel some of the most outstanding questions about the Universe. The mission PI-led program focuses on the massive black holes at the centers of large galaxies ([Section 3.1](#)), compact object populations within galaxies ([Section 3.2](#)), and the diversity of explosive and multi-messenger phenomena to be uncovered in the coming decades ([Section 3.3](#)).

² <https://www.frontiersin.org/research-topics/59532/high-energy-astrophysics-research-enabled-by-the-probe-class-mission-concept-hex-p/overview>



3.1 Goal 1: how do supermassive black holes grow and drive galaxy evolution?

Black holes are extremely efficient at converting rest mass energy into radiation, enabling accreting SMBHs at the centers of galaxies to fundamentally affect and regulate the growth of their hosts. However, the extent of this feedback is uncertain, and whether SMBHs play the leading role or a supporting role is a matter of active study and debate. Understanding this process will require improving both our knowledge of black hole growth and constraining the energy they can provide into their host galaxies.

The X-ray background (Figure 4) represents the summed total of all cosmic X-ray emission and provides the most powerful tool for understanding the cosmic history of black hole growth. Leading models imply that at least 90% of the X-ray background is due to accretion onto SMBHs and this has been largely confirmed in ultra-deep surveys by Chandra and XMM-Newton, reaching months-long exposure times (e.g., Luo et al., 2017), that show the low-energy X-ray sky to be dominated by unobscured AGN. However, while lower-energy X-rays are easily absorbed by intervening gas, higher-energy photons are more penetrating (Figure 1). If most AGN were unobscured, the X-ray background would be relatively flat from 1 to 100 keV. Instead, the 20–30 keV peak of the X-ray background inform us that there is a significant population of obscured AGN missed by soft X-ray surveys. Without accounting for this hidden population, our knowledge of SMBH growth is highly biased.

HEX-P will transform our understanding of how SMBHs grow and drive galaxy evolution, which is a key question of the Astro2020 Decadal Survey (National Academies of Sciences and Medicine, 2023). This goal motivates three science objectives. Objective 1 addresses this question by completing the cosmic census of AGN, finally revealing the full demographics of SMBH growth. Objective 2 addresses both SMBH and galaxy growth by providing a comprehensive survey of SMBH spin, which is an indicator of the interplay between accretion and mergers in galaxy growth. Spin also constrains the energy budget for AGN-driven feedback. Finally, Objective 3 closes a gap in our understanding of the X-ray background by testing the leading physical model for the X-ray

corona to understand the key processes that regulate its temperature and luminosity.

3.1.1 Objective 1: reveal the hidden population of obscured supermassive black holes

Our current understanding of the full census of AGN is highly incomplete. Soft X-ray observatories are strongly biased towards unabsorbed sources (Figure 1), while the shape of the cosmic X-ray background implies approximately half of SMBH growth is obscured. Non-focusing hard X-ray missions resolved just $\sim 2\%$ of the X-ray background at its peak into individual sources (Bottacini et al., 2012), while NuSTAR, the first focusing hard X-ray telescope in orbit, resolved 35% (Harrison et al., 2016). To bring our understanding of the hard X-ray background to the 75–90% levels Chandra and XMM-Newton provide below 6 keV and complete the cosmic census of black hole growth requires improvements in both sensitivity and angular resolution in future hard X-ray telescopes.

The deepest NuSTAR survey detects only 4 sources at an 8–24 keV depth of 5×10^{-14} erg cm $^{-2}$ s $^{-1}$ (Zhao et al., 2021) (throughout, survey depths are reported at a 99% Poisson reliability threshold at 50% area, i.e., 50% of the total survey area reaches that depth or deeper Zhao et al., 2024). At this depth, NuSTAR is reaching the classical confusion limit in the 3–8 keV band, corresponding to 150 sources per deg 2 for the NuSTAR 60" half-power diameter (HPD). Deeper surveys will require improved angular resolution to detect the hard X-ray sources.

In the study presented by Civano et al. (2024), the authors demonstrate via detailed simulations of extragalactic field observations that HEX-P will detect over 1,000 sources at 10–40 keV, compared to the four sources in the deepest NuSTAR survey in the comparable 8–24 keV band (Zhao et al., 2024). Their simulations of a deep and a wide area survey include full instrument models and source detection analysis. They show that with HEX-P, the statistical uncertainty in the measured resolved 10–40 keV X-ray background fraction is predicted to be $\leq 6\%$ for a range of population models (Gilli et al., 2007; Ananna et al., 2019), while the resolved fractions from the models themselves differ by more than 20% in the same energy band.

Deep, broadband extragalactic surveys will, for the first time, uncover the full population of accreting SMBHs and constrain their properties. If HEX-P finds that the heavily obscured fraction is constant with luminosity, this would favor radiation-regulated growth in which radiation pressure dictates the geometry of the obscuring structure (Ananna et al., 2022). If HEX-P instead finds fewer obscured AGN, it might favor models where obscuration occurs primarily in the lowest luminosity AGN, below the survey depth (Lawrence, 1991), or that the SMBH spin rather than obscuration is partially responsible for the characteristic ~ 25 keV peak in the cosmic X-ray background (Vasudevan et al., 2016).

3.1.2 Objective 2: determine the relative importance of accretion versus mergers for SMBH growth

Black holes are the protagonists of one of the most fundamental problems in physics: understanding the complete gravitational collapse of matter to a point that lies within a light-trapping, one-way membrane known as the event horizon. Importantly, only two properties fully define an astrophysical black hole:

its mass M and its angular momentum J , where the latter is commonly reported as the dimensionless spin parameter $a^* = Jc/GM^2$ (where c and G are the speed of light and gravitational constant, respectively); a^* is constrained to values of $-0.998 \leq a^* \leq 0.998$ (Thorne, 1974). Furthermore, mass and spin are fundamentally related. Regardless of its assumed formation channel, a black hole can both increase its mass and change its spin via accretion of matter within its gravitational potential, or via repeated mergers with other black holes. Theoretical models for black hole evolution over cosmic time have specific predictions for how the SMBH mass-spin distribution in the local Universe depends on whether their growth history is dominated by ordered accretion, chaotic accretion or mergers (e.g., Berti and Volonteri, 2008; Dotti et al., 2013; Griffin et al., 2019; Izquierdo-Villalba et al., 2020). Most cosmological simulations predict accretion-dominated growth in lower-mass SMBHs ($< 10^8 M_\odot$), leading to near-maximal expected average spins (e.g., Dubois et al., 2014; Dubois et al., 2021). In semi-analytic models where ordered accretion dominates even in the most massive SMBHs ($> 10^9 M_\odot$), spin parameter values remain high (Sesana et al., 2014), while other models, which follow the hydrodynamics of gas within galaxies, predict an increasing contribution of chaotic accretion and mergers to SMBH growth, leading to lower spin parameter values (Bustamante and Springel, 2019; Beckmann et al., 2024).

Determining whether mergers play a significant role in the growth of SMBHs observed in the local Universe requires a comprehensive spin survey for a sample of SMBHs across a range in black hole mass. While there exists a selection of well-developed methods for measuring SMBH mass, such as reverberation mapping, single-epoch virial estimation or stellar and gas dynamical modelling (see Peterson, 2014, for an overview of the methods), constraining the spin parameter is significantly more challenging. The most effective method is known as X-ray reflection spectroscopy, and is based on measuring the distortion of atomic spectral features by the strong gravitational potential of the SMBH (see Reynolds, 2021, for a review). The hallmarks of reflection are the inner-shell emission lines of iron (Fe K, ~ 6.5 keV), the Fe absorption K-edge (~ 7 keV), and the Compton reflection hump (~ 30 keV), all observed in the broad HEX-P band (Figure 5A). High spin black holes allow for an inner edge of the accretion disk extended closer to the coordinate system origin than their low spin counterparts, leading to greater relativistic distortion of the spectral features. By measuring the degree of this distortion, one can thus infer the inward radial extent of the accretion disk which serves as a proxy for the innermost stable circular orbit and, by extension, black hole spin. Given the resulting width of these features, high spectral resolution of the instrument is not a priority, especially in the absence of absorption features caused by intervening material in the line of sight.³ Instead, a broadband coverage is required to robustly constrain the underlying continuum and isolate the spectral reflection signal. This requirement cannot be fulfilled by soft X-ray observatories whose sensitivity drops rapidly above 8 keV.

³ However, Parker et al. (2022) highlights the importance of Compton reflection hump measurements to disentangle relativistic reflection from disk winds, which imprint absorption features superimposed on the reflection signatures.

Piotrowska et al. (2023) present simulated HEX-P spin parameter measurements for a survey of a 100 AGN selected from the Swift-BAT AGN Spectroscopic Survey (Koss et al., 2017). This sample, complete with published SMBH masses (Koss et al., 2022), includes the brightest hard-X-ray-selected unobscured AGN across the sky observed to date. The study makes use of the Horizon-AGN cosmological simulation to determine spin–mass distributions of SMBHs with different growth histories, which occupy distinct loci in the parameter space. In simulating HEX-P observations, the authors account for measurement uncertainty, model limitations and observational biases, including the strong dependence of radiative efficiency on spin which results in a high-spin bias in flux-limited samples (Figure 5A). The suite of simulated measurements demonstrates that HEX-P robustly distinguishes accretion-dominated models from models where mergers play a significant role in SMBH growth in realistic samples of HEX-P X-ray reflection measurements. As shown by the solid white regions in the right panel of Figure 5, current spin constraints are unable to discriminate between these scenarios, as both SMBH growth histories lie well within the currently permitted spin–mass values. Constraints comparable to HEX-P are not feasible with existing facilities as they would require a year of coordinated XMM-Newton and NuSTAR time.

This large survey, besides answering the Astro2020 key question about how SMBHs grow, also addresses the impact of SMBHs on their host galaxies. With inner disk radii closer to the SMBH, higher spin AGN are also more luminous (Novikov and Thorne, 1973) and thus have a greater energy budget to affect their host galaxy's evolution. Blue-shifted absorption due to fierce, outflowing winds is the clearest indicator of feedback on accretion-disk scales and requires continuum measurements at high energies to constrain line properties (e.g., Fe K is shifted to > 8 keV for winds of $> 0.2c$, requiring sensitivity above 10 keV; Tombesi et al., 2010; Tombesi et al., 2011). Parker et al. (2022) highlight the importance of Compton reflection hump measurements to disentangle relativistic reflection from the signal generated by disk winds. Higher spectral resolution at soft energies is less beneficial as the broad features are easily resolved with typical resolution.

3.1.3 Objective 3: test the leading paradigm for the physics of the X-ray corona

Most of the energetic photons in the universe originate from the X-ray corona, a highly luminous plasma of hot electrons close to the central engine of accreting compact objects (Figure 6). Reverberation and microlensing studies indicate that the corona is extremely compact, extending only a few gravitational radii ($R_g = GM/c^2$) from the central accreting object (neutron star or black hole; Pooley et al., 2007; De Marco et al., 2013; Mosquera et al., 2013; Uttley et al., 2014). Incredibly, the coronae of SMBHs in luminous AGN easily outshine all other high-energy emission in the host galaxy. Per volume, AGN coronae are the most luminous, persistent objects in the universe—and reside partnered with the darkest objects in the universe, black holes. However, beyond a few simple characteristics, the origin and physical mechanisms that govern and power the X-ray corona are poorly understood. HEX-P will fundamentally change this, providing key observations and tests of the leading theoretical

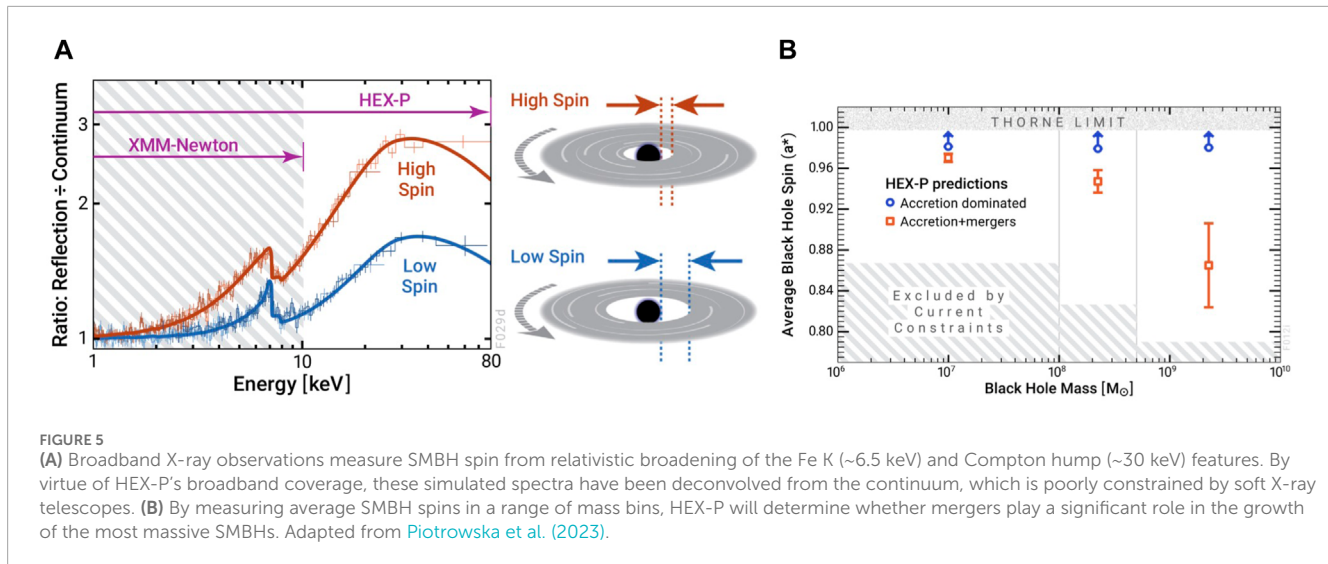


FIGURE 5

(A) Broadband X-ray observations measure SMBH spin from relativistic broadening of the Fe K (~6.5 keV) and Compton hump (~30 keV) features. By virtue of HEX-P's broadband coverage, these simulated spectra have been deconvolved from the continuum, which is poorly constrained by soft X-ray telescopes. (B) By measuring average SMBH spins in a range of mass bins, HEX-P will determine whether mergers play a significant role in the growth of the most massive SMBHs. Adapted from [Piotrowska et al. \(2023\)](#).

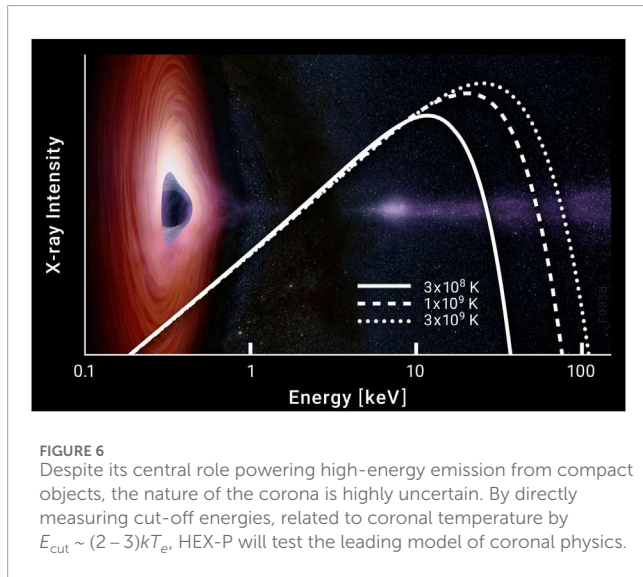


FIGURE 6

Despite its central role powering high-energy emission from compact objects, the nature of the corona is highly uncertain. By directly measuring cut-off energies, related to coronal temperature by $E_{\text{cut}} \sim (2-3)kT_e$, HEX-P will test the leading model of coronal physics.

models. Since the corona dominates the intrinsic X-ray emission of accreting objects, understanding it underlies the AGN population studies in [Sections 3.1.1, 3.1.2](#).

The accretion disk, heated by effective viscosity to high temperatures, produces a blackbody spectrum that peaks at $\sim 0.1 - 1$ keV for stellar-mass compact objects ([Figure 2](#)), and in the UV for SMBHs. Thermal disk photons interact with relativistic electrons in the much hotter corona ($T_e \sim 10^8 - 10^9$ K), increasing the photon energies after repeated inverse Compton scatterings with electrons. The result is a power-law continuum extending up to several hundred keV, and this continuum is more cleanly measured in AGN. For stellar-mass black holes, changes in the X-ray luminosity are also associated with changes in the accretion disk such as the level of the inner-disk truncation, making Galactic binaries poorly suited for this Objective. As coronal photons can only gain so much energy from the relativistic electrons, the power-law-like X-ray spectrum falls off rapidly at a few times the characteristic electron

temperature (referred to as the high-energy cutoff; [Titarchuk and Lyubarskij, 1995](#), and [Figure 6](#)). The electron temperature is the result of the corona's heating-to-cooling balance, where heating takes place magnetically and cooling is set by the number of very high-energy X-ray photons produced. Even a small number of such photons in the compact corona produces copious amounts of electron-positron pairs to share the available thermal energy, cooling the electrons rapidly until a balance is reached. The maximum temperature allowed in this pair-production thermostat model is related to the coronal luminosity.

[Kammoun et al. \(2024\)](#) discusses different tests that can be carried out with a mission like HEX-P to validate this paradigm, along with other coronal studies that could be executed as GO programs. One test focuses on a variable AGN (Test 1; [Figure 7](#), left). These sources provide a powerful tool to test the pair-production thermostat model of the X-ray corona since the model predicts specific tracks along the temperature-luminosity plane. As the luminosity increases, the model predicts that more electron-positron pairs are produced, lowering the plasma temperature. Departures from this relation would indicate incomplete physics, invalidating the model.

Another test concerns luminous AGN (Test 2; [Figure 7](#), right). The pair-production model of the corona also predicts that the highest luminosity sources are cooler since more electron-positron pairs are produced, thereby lowering the coronal temperature, and implying a restricted allowed range of temperature. [Figure 7](#) shows simulations of the luminous sources with expected cut-off energies between 50 and 100 keV. Even if the rest-frame cut-offs were ≥ 200 keV and violating the pair-production model, HEX-P could still constrain the cut-offs to be ≥ 150 keV (90% confidence), which is still unallowed by the pair-production model. Note that high-luminosity AGN are preferentially at high redshift, thereby shifting cut-offs to lower observed energies where the HEX-P sensitivity is higher.

Tests like these would be prohibitive with current facilities as they would require more than 4 Ms of simultaneous XMM-Newton and NuSTAR observations (clock time) but will take only ~ 500 ks for HEX-P.

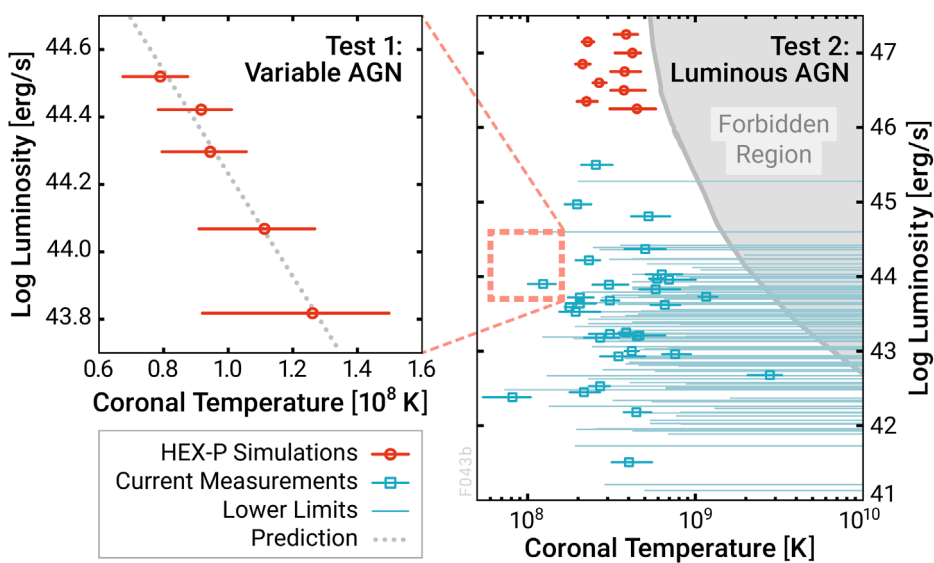


FIGURE 7

HEX-P will validate the pair-production model of the X-ray corona with two tests: measuring how cut-off energy responds to luminosity changes in a variable AGN (Test 1) and observing a sample of luminous AGN (Test 2). Adapted from [Kammoun et al. \(2024\)](#).

3.2 Goal 2: how do binary populations live and die?

Most stars above $8 M_{\odot}$ are in binary systems. The fraction of close binaries depends on both mass and metallicity, driven by the opening chapter of star formation as the proto-stellar disk fragments ([Moe et al., 2019](#)). The story continues as close binaries exchange mass, potentially share a common envelope, have their outer layers stripped off, or even merge. Stripped envelopes and other mass-loss debris surround a dying star and interact with supernova ejecta, causing a diversity of light-curves. Differences imprinted by instabilities in the proto-stellar disk continue to be seen as stellar remnants accrete from a less massive companion and produce an X-ray signal, and as the closest binaries merge and produce a gravitational wave signal in the final chapter of binary evolution. Understanding the extremes of stellar evolution drives major questions highlighted by Astro2020 with implications ranging from cosmic reionization (e.g., [Secunda et al., 2020](#)) to nucleosynthesis (e.g., [Drout et al., 2017](#)). These questions require a range of facilities to answer. Sensitive, broadband X-ray observations, both of our Galaxy and of other galaxies ([Figure 8](#)) to sample a diversity of environments, play an important role by revealing the late stage where one star has died and is feeding on its companion.

Binaries, consisting of a neutron star or black hole accreting from a stellar companion (i.e., X-ray binaries), and their lower mass cousins with an accreting white dwarf (i.e., cataclysmic variables; CVs), provide unique constraints on how multiplicity affects massive star evolution, as well as on the physics of accretion and its environmental impact. While Chandra and XMM-Newton have surveyed nearby galaxies for more than two decades, such work has been below 10 keV which limits insight into the underlying astrophysics. Advances will require higher energy X-rays to access spectral signatures that distinguish accreting compact object types

(e.g., neutron stars versus black holes), measure CV white dwarf mass, and determine accretion state ([Remillard and McClintock, 2006](#)). State transitions in X-ray binaries, boundary layer emission from accreting neutron stars, and accretion columns in pulsars all have distinguishable spectral shapes above 10 keV. These questions motivate Objective 4, described next.

3.2.1 Objective 4: determine how different galactic environments build binary systems with compact objects

[Mori et al. \(2024\)](#) presents simulated HEX-P surveys of the central regions of the Milky Way, while [Lehmer et al. \(2023\)](#) presents simulated HEX-P surveys of four nearby galaxies (M31, Maffei 1, NGC 253, and NGC 3310). These studies show how HEX-P observations can be used to investigate how X-ray populations depend on environment and metallicity. Milky Way studies are sensitive to CVs and X-ray binaries, while most detected extragalactic sources will be X-ray binaries. HEX-P's broadband response, high timing resolution, and high angular resolution will enable unprecedented sensitivity for the detection of pulsations from sources in crowded environments where traditional timing-dedicated mission (with high effective areas but little imaging capabilities) would struggle, such as the Galactic Center ([Mori et al., 2024](#)) and nearby Galaxies ([Bachetti et al., 2023](#)).

3.2.1.1 Milky way

The Galactic Center survey will cover a total area of ≥ 1 deg². The simulations by [Mori et al. \(2024\)](#), based on extrapolating known Chandra sources to higher energy assuming 15–30 keV thermal spectra (typical of mCVs), show that HEX-P will detect > 1000 sources within 30' of Sgr A* in the 2–20 keV band. For comparison, NuSTAR, with its 60" HPD, provides the current sharpest images of the X-ray sky above 10 keV but is heavily confused and suffers from stray light (both limitations that HEX-P will overcome).

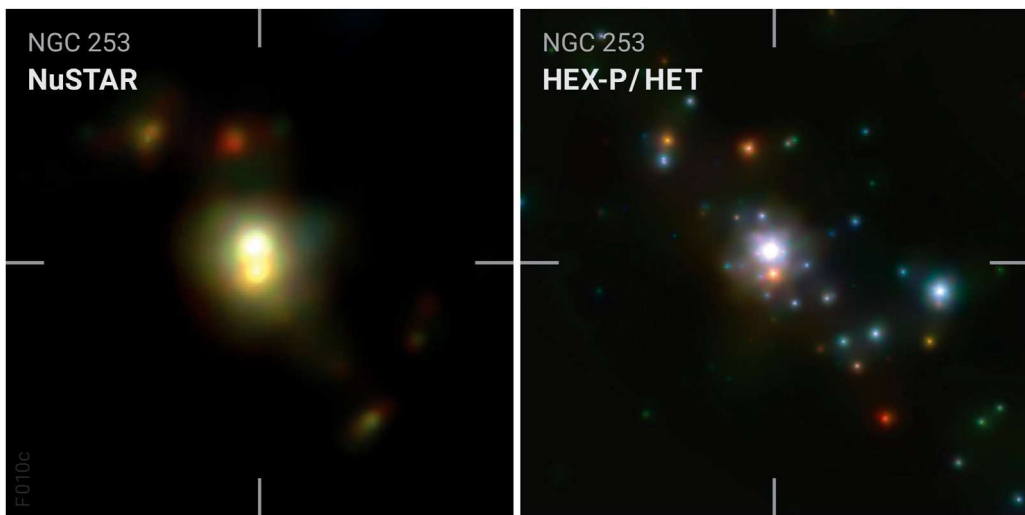


FIGURE 8
HEX-P will provide the first sensitive broadband studies of high-energy populations in the nearby universe. Adapted from [Lehmer et al. \(2023\)](#).

The NuSTAR Galactic Center survey covered a similar area and detected only 66 sources above 10 keV ([Hong et al., 2016](#)). HEX-P will be transformative, providing data with sufficient angular resolution, spectral range, and sensitivity to classify the rich binary populations in the center of our Galaxy and study how their properties depend on their environment. The nuclear star cluster in the central 10 pc around Sgr A* is the densest stellar environment in the Galaxy. While NuSTAR discovered diffuse hard X-ray emission from this region ([Perez et al., 2015](#)), HEX-P is needed to resolve that emission into individual sources, enabling confirmation of the predicted population of tightly bound black hole binaries in the innermost regions suggested by low energy data ([Mori et al., 2021](#)), or finding a central concentration of pulsars, which would have implications for the origin of the Galactic Center GeV excess detected by Fermi ([Gautam et al., 2022](#)). Since detecting radio pulsars in this region is challenging due to the large radio dispersion measure, HEX-P is particularly well suited for finding pulsars near Sgr A*.

3.2.1.2 Nearby galaxies

Extragalactic surveys provide additional insight into extreme stars and multiplicity by accessing a wider range of environments. Chandra has been surveying nearby galaxies for over two decades, but its X-ray binary studies are hampered by its limited 0.5–8 keV energy range which fails to robustly separate neutron star and black hole X-ray binary populations ([Figure 9](#), left). Rather than observing more galaxies or increasing spectral resolution, the biggest scientific gains will come from broader spectral coverage, which breaks this degeneracy ([Figure 9](#), right; [Wik et al., 2014](#)) and identifies accretion states (e.g., soft and hard states; [Figure 2](#)). Characteristic pulsations or flaring activity indicative of a neutron star (e.g., Type I and II X-ray bursts) provide additional classification information.

Detailed HEX-P simulations based on Chandra data, including an assumed distribution of neutron star and black hole binaries, realistic spectral models, and confusion from sources below the detection limit, predict over 200 X-ray binaries will be detected in

the nearby galaxy survey, including > 130 detected above 12 keV ([Lehmer et al., 2023](#)). This is an order of magnitude more than current hard X-ray studies, which suffer from source confusion ([Figure 8](#)) and fail to reach typical HMXB depths. Simulations show that HEX-P will robustly characterize compact object types and accretion states in extragalactic environments ([Figure 9](#)), enabling the first comprehensive study of binary populations across a wide range of galactic environments, thereby providing key data to constrain high-mass star formation and stellar evolution models.

3.3 Goal 3: what powers the diversity of explosive phenomena across time and multi-messenger domains?

A new generation of time-domain and multi-messenger (TDAMM) facilities will open tremendous discovery space across astrophysics in the coming decade. With deep, multi-color images, Rubin Observatory will profoundly transform our view of the variable sky, while upgraded gamma-ray, neutrino, and gravitational wave facilities transform our view of particle acceleration and compact object mergers. A unifying theme in the diversity of phenomena to be uncovered is their energetic nature, implying they are likely X-ray emitters. However, the prospects for sensitive X-ray follow-up are uncertain. The two flagship-class X-ray missions, Chandra and XMM-Newton, are both in their third decade in orbit, have restricted fields of regard, and lack the agility to regularly and rapidly respond to targets of opportunity (ToOs). To leverage the full potential of TDAMM investments, a sensitive and agile X-ray facility is required. Angular and spectral resolution are less critical than simultaneous broadband sensitivity.

HEX-P is designed to provide the requisite sensitivity and agility, and this priority science area motivates two objectives: understanding the most powerful Galactic accelerators (factories for neutrinos, cosmic rays, and gamma-rays), and providing a community resource for exploring the dynamic universe.

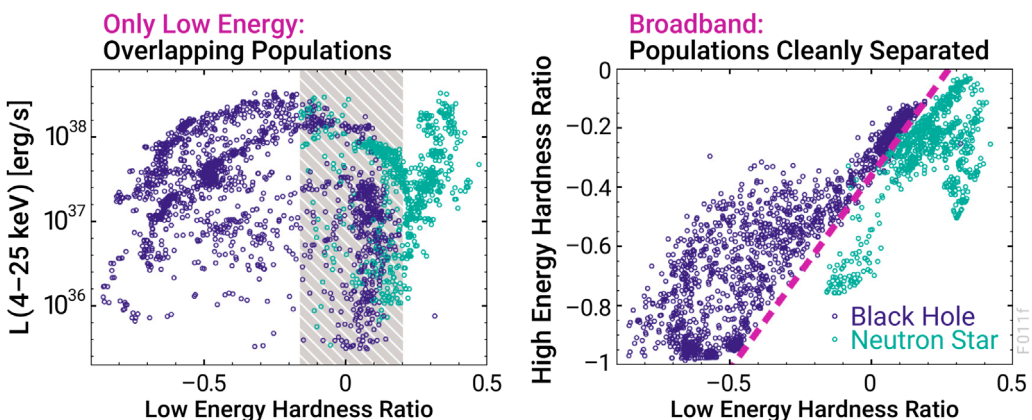


FIGURE 9

Broadband X-ray data cleanly separates black hole and neutron star X-ray binaries. Hardness ratios (HRs) use bands at 4–6 (S), 6–12 (M), and 12–25 (H) keV, and data is from a handful of bright Galactic binaries observed by RXTE. HEX-P will extend these studies into the crowded Milky Way center and to nearby galaxies. Adapted from [Lehmer et al. \(2023\)](#).

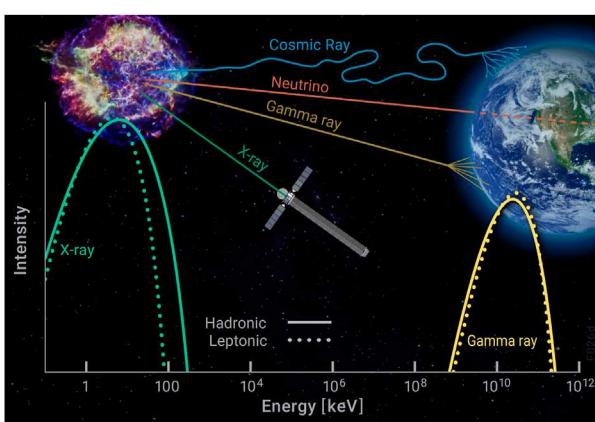


FIGURE 10

HEX-P will study the most energetic particle acceleration sites in the Galaxy, producing PeV cosmic rays, 100 TeV neutrinos, ultra-high energy gamma-rays, and X-rays. Hard X-ray data (> 10 keV) provide unique information to constrain accelerator mechanisms.

3.3.1 Objective 5: find the sources of the most energetic cosmic rays and neutrinos in our galaxy

Cosmic rays, charged extraterrestrial particles that continuously bombard the Earth's atmosphere (Figure 10), exhibit a power-law flux distribution over more than 12 orders of magnitude in energy. Low energy cosmic rays are primarily solar protons, while the most energetic are primarily extragalactic. At the “knee” of the distribution near 10^{15} eV = 1 PeV, the particles are believed to be primarily Galactic from “PeVatron” sources, the most energetic acceleration sites in the Milky Way Galaxy. Understanding these extreme sources requires a multi-messenger approach, addressing the physics of supernova shock waves, pulsar wind nebulae, and other exotic environments, with information from radio, X-rays, gamma-rays, and neutrinos (Figure 10).

Understanding Galactic PeVatron sources requires access to the 40–80 keV energy band. Since cosmic rays are charged particles, their trajectories are deflected by interstellar magnetic fields, disguising their origins. Energetic cosmic ray electrons inverse-Compton scatter ambient photons to produce very high-energy emission, up to ~ 100 TeV (Harding, 1996). However, modeling this emission requires knowledge of the seed photon population (e.g., cosmic microwave background, nearby synchrotron, or nearby thermal sources), and the highest energy emission is affected by quantum electrodynamical effects i.e., Klein-Nishina suppression (Klein and Nishina, 1929). Energetic cosmic-ray electrons also emit synchrotron photons in the X-ray to MeV band. Since this emission reflects the particle spectrum more directly, it provides a key tool for investigating particle acceleration and transport (Reynolds, 2016; Burgess et al., 2022; Mori et al., 2022). A strategic observational campaign, including a list of proposed HEX-P targets, is discussed in detail in [Mori et al. \(2023\)](#).

These targets have significant scientific value beyond the scientific goal of understanding particle acceleration. For example, the morphology and kinematics of the ^{44}Ti emission at 78 keV in supernova remnants is a powerful diagnostic of supernova explosion physics. The capabilities offered by HEX-P in addressing this and other interesting problems on nuclear astrophysics are discussed at length in [Reynolds et al. \(2023\)](#).

3.3.2 Objective 6: provide a community resource to explore the dynamic universe across the X-ray band

HEX-P will be an essential resource in the 2030s, providing sensitive high-energy access to explore explosive events and monitor variable sources with other facilities. HEX-P will devote a fraction of its exposure time to unanticipated transient observations triggered by the community. This time could be considered a form of community GO access, though HEX-P conservatively assesses it as PI-led time since it is allocated by the PI rather than NASA. This will enable HEX-P to provide more flexible and rapid response

to community needs. A few example potential programs are discussed below.

3.3.2.1 Gravitational wave mergers

To date, the binary neutron star merger GW170817 remains the only gravitational wave event with a clear electromagnetic counterpart (Margutti and Chornock, 2021) and this unique event prompted the most intense multiwavelength observational campaign in recent times (Abbott et al., 2017). X-ray observations revealed a slowly rising source appearing 9 days after the merger and peaking at 6 months, indicating that the merger produced a relativistic structured jet whose core was oriented 2° from the line of sight, consistent with an off-axis short gamma-ray burst. The jet structure likely results from the jet interaction with the merger ejecta.

As described in the study by Brightman et al. (2024), HEX-P follow-up of gravitational wave merger counterparts identified by other facilities will provide broadband X-ray light-curves to probe ejecta properties such as energy and angular structure, informing which mergers can launch ultra-relativistic jets (e.g., Sun et al., 2022), and help disambiguate binary neutron star mergers from mergers of neutron stars with black holes. This is a rich, largely unexplored scientific landscape which touches on a wide range of physics from binary star evolution to relativistic jet physics and nucleosynthesis. Determining the merger product constrains the neutron star equation of state, with implications ranging from heavy element abundances to biases in cosmological parameters (Burns, 2020). Theory also predicts that lower mass binary neutron star mergers can form long-lived supermassive neutron star remnants, detectable from the bright hard X-ray emission produced from a resultant magnetar wind nebula (Murase et al., 2018).

3.3.2.2 Fast blue optical transients (FBOTs)

Time-domain surveys are now uncovering new classes of rapidly evolving transients that challenge our notions of energetic events and stellar death. In this rapidly evolving landscape, FBOTs stand out as particularly intriguing. Their short timescales, luminosities that can exceed superluminous supernovae, and lack of UV line blanketing imply a power source other than standard supernova models powered by ^{56}Ni radioactive decay. AT2018cow illustrates the importance of broadband X-ray data for understanding transient phenomena. NuSTAR data taken a week after discovery (Figure 11) revealed excess high-energy emission with properties unprecedented among previous astrophysical transients (Margutti et al., 2019). The high-energy AT2018cow spectrum shows signatures of central engine emission reflecting off spherical optically thick material, potentially a funnel formed by a powerful accretion flow. The high inferred environmental density disfavors an alternative hypothesis that AT2018cow was due to the tidal disruption of a star by an off-center intermediate mass black hole (Perley et al., 2019). This work highlights the importance of access to the hard X-ray range, which HEX-P provides for studying the dynamic universe.

3.3.2.3 Embedded events

Many explosive events are obscured at early times, from circum-burst material, stellar ejecta, or because the event has occurred in a dense environment. Such emission will be highly absorbed,

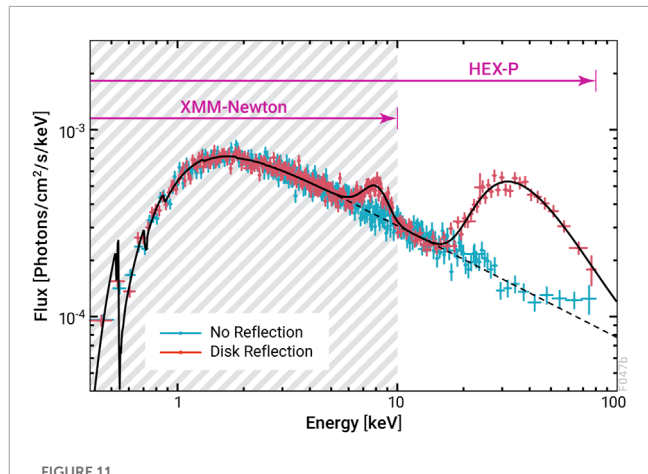


FIGURE 11

Broadband HEX-P data reveals components missed by low-energy observatories. This simulated HEX-P spectrum of AT2018cow, based on NuSTAR observations (Margutti et al., 2019), reveals reflection from a newly formed central engine. Soft X-ray observations only constrain the underlying power-law continuum, with ambiguous hints of Fe K emission.

preferentially detected in hard X-rays, and changes in the absorbing column reveal the structure of that material. For example, NuSTAR observations of SN 2023ixf in the Pinwheel Galaxy initially revealed a highly absorbed source just 4 days after the supernova explosion, at a time when Swift only obtained upper limits (Grefenstette et al., 2023). Observations a week later revealed a substantially lower gas column, implying the absorption was due to a thin shell of circumstellar material, likely ejected in the final few to 10 years of the star's life. With more rapid and more sensitive ToO observations, HEX-P's broadband capabilities open a new window into the final stages of stellar evolution, as well as events occurring in dense environments.

3.4 Potential for general observer (GO) programs

Examples of potential GO programs that emphasize the range of science enabled by HEX-P are described below. As with the PI-led science described above, each of these programs has been studied in detail and reported in the indicated papers from this Research Topic.

3.4.1 Accretion onto stellar-mass black holes

Accretion of matter onto a black hole is one of the most efficient mechanisms to produce energetic radiation. While SMBHs in centers of galaxies logically provide the most extreme environments, stellar-mass black holes are arguably the best laboratories to understand the physics of accretion and the interaction between radiation and matter in the strong gravity regime. Stellar-mass black holes in binary systems with stellar companions, also known as X-ray binaries, are the primary candidates for such studies. There are close to 30 of these systems confirmed in our Galaxy. They are abundantly bright in X-rays, and relatively nearby (\sim few kpc). Their much smaller size compared to SMBHs also means that they regularly display a rich phenomenology on human time scales;

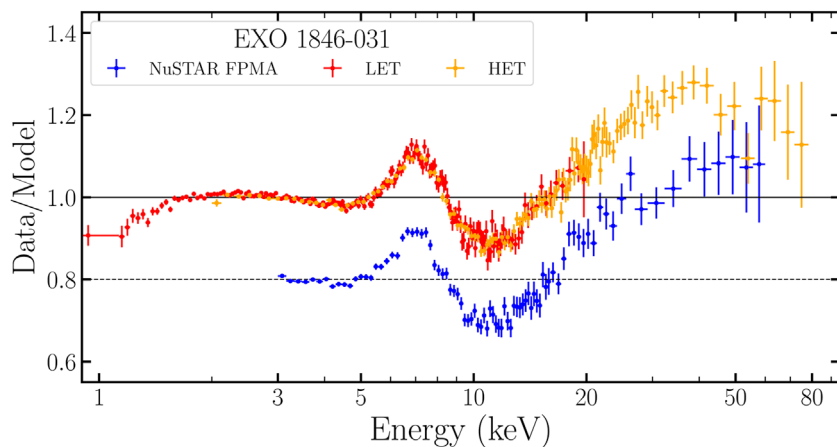


FIGURE 12

X-ray spectra of the black hole binary EXO 1846–031 observed by NuSTAR (blue), and simulated with HEX-P LET (orange) and HET (red). HEX-P's increased sensitivity and broader energy coverage enables better constraints on the physical properties of the system. Adapted from [Connors et al. \(2024\)](#).

i.e., weeks to months, rather than years to megayears ([Tanaka and Lewin, 1995](#); [Remillard and McClintock, 2006](#)). Thus, high signal-to-noise data, combined with accelerated evolution, makes black-hole binaries (BHBs) the premier sources to learn about black holes and their effects on space-time, matter and radiation.

[Connors et al. \(2024\)](#) present a study that illustrates the capabilities of HEX-P in measuring the evolving structures of accretion flows in BHBs observed at much lower luminosities than achieved with current facilities. Their simulations demonstrate that HEX-P can accurately measure the inner radius of the accretion disk via reflection spectroscopy at luminosities below 0.1% Eddington ([Figure 12](#)). For brighter sources, HEX-P's observations will provide unprecedented data to probe the properties and indirect measurements of the geometry of the X-ray corona.⁴ Detailed broadband studies of systems in nearby galaxies could be achieved for black holes accreting above the Eddington limit, which would expand the repertoire of sources available, possibly including those from different populations that have not yet been studied.

3.4.2 Jet physics in blazars

A fraction of accreting SMBHs launch powerful relativistic jets that can reach kpc, even Mpc scales. When the jets align with our line of sight, they appear boosted, producing bright, highly variable multi-band and multi-messenger emission. HEX-P is poised to answer many open questions about what powers these cosmic monsters. HEX-P's ability to pinpoint fast variability (comparable to the system light-crossing time) simultaneously from 0.2–80 keV will reveal particle acceleration mechanisms taking

place in these jets, such as magnetic reconnection and shocks. The instrument's broadband sensitivity will enable us to disentangle leptonic and hadronic emission mechanisms ([Figure 10](#)), potentially detecting proton-induced cascades associated with neutrino emission. Moreover, its sensitivity is paramount to detect a large fraction of the highest redshift ($z > 4$) jets, essential to trace the evolution of jets and SMBHs into the early universe. As described by [Marcotulli et al. \(2023\)](#), HEX-P will also spatially resolve blazar and radio galaxy jets from core emission for the first time above 10 keV ([Figure 13](#)), thereby measuring jet spectral cut-offs and constraining the maximum energy of the particle population. Since blazars are strong, multi-messenger and time-variable sources, HEX-P blazar science has strong synergies with many facilities expected to be in operation in the early 2030s, including NASA's IXPE (X-ray; [Weisskopf et al., 2022](#)), COSI (γ -ray; [Tomsick et al., 2023](#)), and UVEX (ultraviolet; [Kulkarni et al., 2021](#)) missions, and the ground-based IceCube (neutrino; [IceCube Collaboration, 2005](#)) and CTAO (γ -ray; [Hofmann and Zanin, 2023](#)) facilities.

3.4.3 Equation of state (EoS) of ultradense matter

With interior densities several times higher than atomic nuclei and size scales of 10–20 km, neutron stars are the densest objects that persist in Nature, and they exist on the verge of imploding into a black hole. Understanding how matter behaves under these extreme conditions is encapsulated in the EoS, relating the mass and radius of the neutron star ([Tolman, 1939](#); [Oppenheimer and Volkoff, 1939](#)), and it is best determined through astronomical measurements ([Lattimer, 2011](#)).

Each method of determining the EoS of ultradense matter has underlying systematic uncertainties and probes different regions of the mass-radius parameter space ([Figure 14](#)). The firmest constraints require multiple approaches. Pulsar timing studies assume simplistic geometrical models (i.e., not physically motivated) of temperature across the neutron star surface (e.g.; [Miller et al., 2019](#)), while gravitational wave studies provide tight radius constraints with

⁴ While more precise and direct measurements of the geometry of inner accretion flows can be achieved by facilities such as the Event Horizon Telescope (EHT; [Doeleman et al., 2009](#)) or Gravity+ ([Gravity+ Collaboration et al., 2022](#)), their observations are limited to a few selected sources.

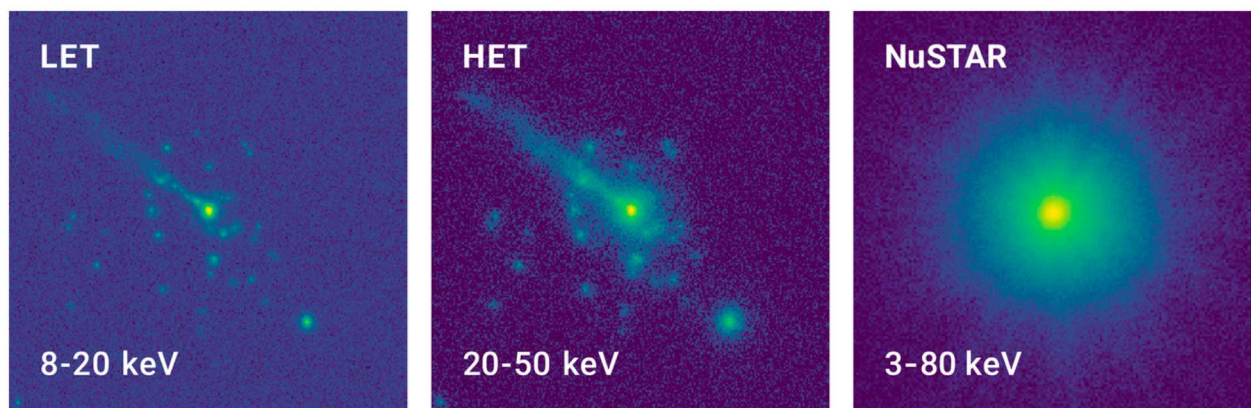


FIGURE 13
HEX-P will resolve the extended jet and point sources above 10 keV, like the one observed in Centaurus A. Adapted from [Marcotulli et al. \(2023\)](#).

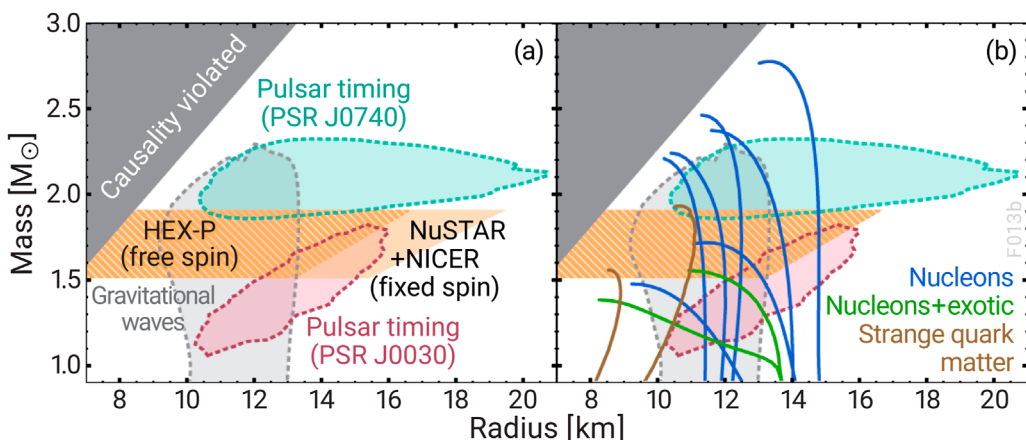


FIGURE 14
(A) Mass and radius constraints from reflection modeling compared to neutron star gravitational wave events and NICER pulsar lightcurve modeling. **(B)** Same as panel **(A)** but including a family of EoS theoretical predictions. Adapted from [Ludlam et al. \(2023\)](#).

poor mass constraints ([Raaijmakers et al., 2021](#)). Broadband X-ray studies covering 0.5–50 keV robustly measure continuum and reflection features, thereby providing the radius of the inner edge of the accretion disk and placing a strong, physical upper limit on the neutron star size ([Ludlam et al., 2022](#)). However, current measurements from coordinated NICER and NuSTAR observations require fixing the neutron star spin (typically assuming no rotation). The study by [Ludlam et al. \(2023\)](#) shows how the improved sensitivity of HEX-P will enable robustly solving for neutron star spin, thereby providing tighter radial constraints with less systematic bias.

3.4.4 Accretion and other physical processes in strong magnetic fields

With magnetic fields reaching typical strengths of $\sim 10^{12}$ G in high-mass X-ray binary systems and $\sim 10^{15}$ G in magnetars, accreting neutron stars provide a unique laboratory to study the extreme physics of accretion in the presence of strong magnetic fields. Neutron star magnetic field strengths are orders of magnitude higher

than the strongest magnetic fields achieved in terrestrial laboratories ($\sim 5 \times 10^5$ G). In high-mass binary systems, magnetic field pressure disrupts the inflow of the accreting material, channeling matter onto the magnetic poles. Since the neutron star rotates, radiation is released in a highly anisotropic manner, producing pulsing X-ray emission whose broadband study informs the plasma physics as well as the interaction of radiation with ultra-strong magnetic fields. Magnetars are also useful probes of the physics of the interaction of radiation with ultra-strong magnetic fields, but like some isolated neutron stars, that they are not thought to be accreting. The predictions for HEX-P's unique capabilities in addressing important questions about the physics of magnetars and other isolated neutron stars are extensively discussed in [Alford et al. \(2024\)](#).

Due to the very high magnetic field present in magnetars, electron motion perpendicular to the magnetic field lines becomes quantized, leading to a resonance proportional to the magnetic field strength. This produces absorption-like cyclotron resonant scattering features, or simply cyclotron lines, at 5–100 keV. Cyclotron lines represent the most direct way to probe magnetic

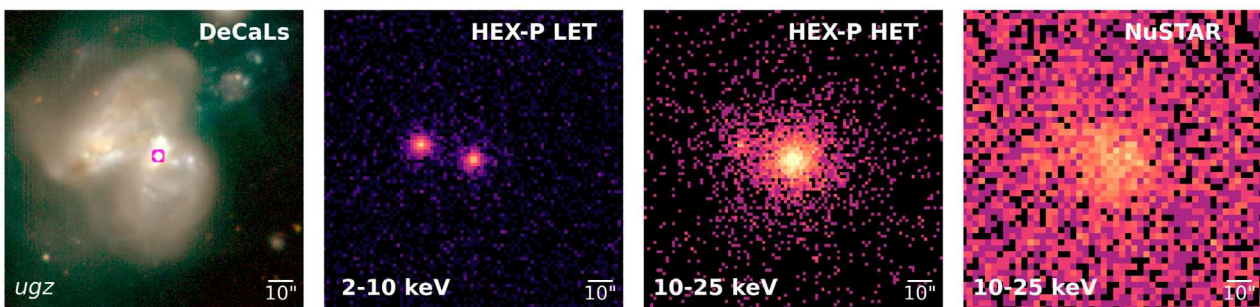


FIGURE 15

HEX-P will resolve obscured AGN in galaxy mergers, such as Arp-299 shown here. Note that the low-energy LET observation finds both components to be comparably bright, while the high-energy HET reveals the western component to be significantly brighter and heavily obscured. Adapted from Pfeifle et al. (2023).

field strengths on or close to the neutron star surface, and they have been detected in about 40 sources (Staubert et al., 2019). Detecting fundamental lines and harmonics, and measuring their dependence on pulsar phase and luminosity, provides crucial insight into the accretion physics, including its geometry, electron bulk motion, turbulence, temperature distribution, and plasma conditions (Kreykenbohm et al., 2002).

Bachetti et al. (2023) presents a comprehensive study of potential HEX-P programs studying ultra-luminous X-ray sources (ULXs), at least some of which are neutron stars accreting at extreme rates, up to ~ 500 times the Eddington limit (e.g., Bachetti et al., 2014; Fürst et al., 2016; Israel et al., 2017). Cyclotron lines provide the most direct measurement of ULX magnetic field strengths, which may be the key factor enabling their extreme luminosities. HEX-P will also be able to detect and study the radiatively-driven winds discovered in ULXs (Pinto et al., 2016), providing essential information on super-Eddington accretion and unveiling the origin of their surrounding 100-pc interstellar bubbles (Gúrpide et al., 2022).

3.4.5 SMBH activity in merging galaxies

HEX-P is an essential tool for studying SMBH growth. Merging galaxies offer one of the most dramatic channels for galaxy evolution, driving inflows of gas into galactic nuclei and potentially fueling both star formation and central SMBH activity. Dual AGN in late-stage mergers with nuclear pair separations < 10 kpc are ideal candidates to study SMBH growth since they coincide with the most transformative period for galaxies. However, since mergers are also associated with severe gas and dust obscuration (Koss et al., 2018; Blecha et al., 2018; De Rosa et al., 2019), dual AGNs are difficult to confirm and study, particularly with soft X-ray observatories. Hard X-rays offer a powerful tool to penetrate the dense obscuring media predicted to surround dual AGN in late-stage mergers (Figure 15). To date, only a handful of the brightest and closest systems have been studied at these energies due to the demanding instrument requirements involved. HEX-P enables, for the first time, the ability to spatially resolve hard X-ray counterparts of closely separated ($\sim 2 - 5''$) dual AGN.

The study reported by Pfeifle et al. (2023) shows via simulations that HEX-P will probe dual AGNs in late-stage mergers (< 10 kpc)

out to $z \sim 0.1$, and intermediate-stage mergers (~ 30 kpc) out to $z \sim 0.3$. This is a dramatic improvement over NuSTAR and enables science that cannot be done with a soft X-ray observatory. HEX-P will transform our understanding of the role of AGN triggering and AGN feedback during galactic mergers.

3.4.6 The circum-nuclear environment of growing SMBHs

The vast majority of accretion onto SMBHs takes place within a dense obscuring fortress of gas and dust. This circum-nuclear obscurer connects interstellar space to the accretion disc, and is known to evolve with both the accretion power of the central engine as well as the age of the Universe (e.g., Ueda et al., 2014; Buchner et al., 2014; Ananna et al., 2019). Thus a complete understanding of SMBH growth requires intricate knowledge of the structure and dynamics of the circum-nuclear environment surrounding AGN.

However, our current knowledge of the obscurer is fundamentally incomplete. Estimates of heavily obscured AGN space densities is unconstrained with observations typically suggesting that anywhere between $\sim 10\%-50\%$ of all SMBH activity takes place within material exceeding the Compton-thick limit (column density $N_H > 10^{24} \text{ cm}^{-2}$; e.g., Ricci et al., 2015; Kammoun et al., 2020; Torres-Albà et al., 2021). Geometrical parameters describing the obscurer's structure, such as covering factor, impose subtle changes on the observed hard X-ray spectrum of obscured AGN that NuSTAR can only begin to identify in a handful of brightest targets (e.g., Buchner et al., 2021). Furthermore, advances driven by NuSTAR have demonstrated that the obscurer is not static, but predominantly dynamic in nature (e.g., Baloković et al., 2021; Marchesi et al., 2022; Torres-Albà et al., 2023).

Boorman et al. (2023) present a series of simulations to show the exciting ways in which HEX-P will advance our understanding of the circum-nuclear environment surrounding AGN. Dramatic advances in sensitivity driven by reduced backgrounds and enhanced angular resolution will increase the available volume for robustly confirming heavily obscured accretion by more than an order of magnitude. By providing broadband X-ray spectral constraints on select AGN with precise black hole mass estimates, HEX-P will drive the development

of new physically-motivated models that are capable of describing the geometrical structure of the obscurer in relation to the accretion power of the central engine. Also, the strictly simultaneous soft and hard X-ray spectral constraints provided by HEX-P will enable new insights into the dynamical nature of the obscurer via monitoring campaigns. [Boorman et al. \(2023\)](#) show that the passband of HEX-P is sufficient to disentangle intrinsic flux variations from structural changes of the obscurer to high precision, a task virtually impossible with current instrumentation and cadences.

4 Synergies with other facilities

The HEX-P mission will offer powerful synergies with key astronomical facilities expected to be operational in the 2030s, advancing our understanding of the high-energy universe across multiple wavelengths and observational techniques.

HEX-P's high-energy X-ray capabilities will greatly complement JWST's observations in the infrared, allowing for simultaneous studies of the most distant and energetic objects in the universe. While JWST probes the formation of galaxies, stars, and black holes in the early universe through infrared light, HEX-P will trace the high-energy processes occurring within these systems, such as supermassive black hole growth and powerful galactic winds. In obscured AGN, JWST can map the IR emission from the obscuring material, while HEX-P sees the strong X-ray emission from the central engine. Together, they will provide a comprehensive view of the formation and evolution of galaxies and the role of high-energy phenomena in shaping cosmic structure.

In the UV band, the Ultraviolet Explorer (UVEX) and HEX-P will form a powerful combination, covering the ultraviolet and X-ray regimes to study hot, energetic environments like the atmospheres of neutron stars, black hole accretion disks, and supernova remnants. UVEX will capture emissions from ionized gas and hot stars in the ultraviolet, while HEX-P will observe the high-energy processes at play.

In the soft X-rays, HEX-P will complement NewAthena's focus on the soft X-ray band, extending the observational window into the hard X-ray regime. This synergy will allow for simultaneous, multi-band X-ray observations of black holes, galaxy clusters, and neutron stars, revealing more about their energetic environments and evolution. The unrivaled energy resolution of the X-IFU microcalorimeter in NewAthena will reveal the detailed structure of atomic features with unprecedented precision, while HEX-P's broadband coverage will be crucial to uniquely constrain the continuum emission to very high energies.

At very high energies (e.g., gamma rays), HEX-P will synergize with key observatories like COSI, IceCube, and CTAO, creating an observational network to explore the most energetic and extreme phenomena in the universe. This includes detecting processes like gamma-ray bursts (GRBs), supernova explosions, and positron annihilation events with COSI (soft gamma rays); provide X-ray counterparts to IceCube's neutrino detections from the most energetic cosmic accelerators, such as blazars, active galactic nuclei (AGN), and gamma-ray bursts; and complementing CTAO's focus on very-high-energy gamma rays from cosmic sources like AGN, pulsar wind nebulae, and supernova remnants.

As we adventure in the new era of gravitational wave detections, HEX-P will complement Advanced LIGO and LISA's gravitational wave detections by providing rapid follow-up of high-energy X-ray observations of black hole mergers and neutron star collisions. Together, these missions will offer a multi-messenger view of extreme cosmic events, enabling detailed studies of their dynamics and environments.

In the time-domain arena, proposed missions like THESUS (Transient High-Energy Sky and Early Universe Surveyor) and the GAMOW Explorer would deliver new triggers for transient sources. While THESUS will focus on detecting and localizing transient sources like gamma-ray bursts (GRBs) and outbursting X-ray binaries like black holes and neutron stars, HEX-P will provide deeper high-energy follow-up observations, characterizing their X-ray emission. Moreover, by working in tandem with GAMOW's gamma-ray observations, HEX-P will extend the energy range of investigation for phenomena like GRBs and active galactic nuclei (AGN). This collaboration will enable a more comprehensive analysis of the most energetic processes in the universe.

Through all these and many other collaborations, HEX-P will play a pivotal role in multi-messenger and multiwavelength astrophysics, helping to unlock new insights into the fundamental physics of the cosmos.

5 Final remarks

The low-energy capabilities of HEX-P build on the successes of the two current flagship X-ray missions, both soft X-ray observatories that launched in 1999. HEX-P combines greater effective area than Chandra with improved angular resolution over XMM-Newton. HEX-P also has an improved agility to respond to ToO requests, thereby retrieving data prioritized by Astro2020. Broadband X-rays reveal obscured sources, access new spectral features, and improve modeling of soft-band data. Since 2021, > 50% of NuSTAR observations have been coordinated with soft X-ray satellites (i.e., Chandra, XMM-Newton, IXPE, Swift, NICER, XRISM) to provide simultaneous broadband coverage, and a similar reliance on HET is expected for future soft X-ray observatories, such as NewAthena. With sensitivity to 80 keV, HEX-P shrinks the gap between X-ray and gamma-ray facilities, complementing NASA's Compton Spectrometer and Imager (COSI; 0.2–5 MeV; launch in 2027) and the Cherenkov Telescope Array Observatory (CTAO; 0.02–300 TeV; ground-breaking in 2024). Finally, HEX-P provides essential data to probe TDAMM sources to be found in the 2030s by gravitational wave, neutrino, cosmic ray, and photon facilities (e.g., Rubin, Roman, UVEX, and JWST). To leverage the full potential of TDAMM investments, we require a sensitive and agile X-ray facility in the 2030s. Rather than improving angular resolution or spectral resolution, the biggest scientific gains come from simultaneous broad, sensitive spectral coverage.

The work summarized in this paper has been largely led by members of the high-energy astrophysics community, most of whom are not Co-investigators of the HEX-P mission proposal. This exemplifies the strong interests and needs for a facility with capabilities like those in HEX-P. Furthermore, while the science cases discussed in this collection of papers cover the core science of the mission, they do not represent a complete or

comprehensive list of topics that a mission like HEX-P can achieve. The potential for new science reaches far beyond these themes, and perhaps the most promising discoveries are those that will come unexpectedly.

Data availability statement

The raw data supporting the conclusion of this article will be made available by the authors, without undue reservation.

Author contributions

JG: Writing-original draft, Writing-review and editing. DSt: Writing-original draft, Writing-review and editing. KrM: Writing-original draft, Writing-review and editing. MS: Writing-original draft, Writing-review and editing. BG: Writing-original draft, Writing-review and editing. MA: Writing-original draft, Writing-review and editing. JA: Writing-original draft, Writing-review and editing. AA: Writing-original draft, Writing-review and editing. MaB: Writing-original draft, Writing-review and editing. MiB: Writing-original draft, Writing-review and editing. RB: Writing-original draft, Writing-review and editing. SB: Writing-original draft, Writing-review and editing. DB: Writing-original draft, Writing-review and editing. PB: Writing-original draft, Writing-review and editing. MuB: Writing-original draft, Writing-review and editing. JB: Writing-original draft, Writing-review and editing. EB: Writing-original draft, Writing-review and editing. C-TC: Writing-original draft, Writing-review and editing. FC: Writing-original draft, Writing-review and editing. JC: Writing-original draft, Writing-review and editing. RC: Writing-original draft, Writing-review and editing. MD: Writing-original draft, Writing-review and editing. LG: Writing-original draft, Writing-review and editing. PD: Writing-original draft, Writing-review and editing. PF: Writing-original draft, Writing-review and editing. AG: Writing-original draft, Writing-review and editing. MG: Writing-original draft, Writing-review and editing. SG: Writing-original draft, Writing-review and editing. FH: Writing-original draft, Writing-review and editing. EK: Writing-original draft, Writing-review and editing. GL: Writing-original draft, Writing-review and editing. BL: Writing-original draft, Writing-review and editing. AL: Writing-original draft, Writing-review and editing. RL: Writing-original draft, Writing-review and editing. SM: Writing-original draft, Writing-review and editing. LM: Writing-original draft, Writing-review and editing. RM: Writing-original draft, Writing-review and editing. MeM: Writing-original draft, Writing-review and editing. AnM: Writing-original draft, Writing-review and editing. MaM: Writing-original draft, Writing-review and editing. KaM: Writing-original draft, Writing-review and editing. AlM: Writing-original draft, Writing-review and editing. KN: Writing-original draft, Writing-review

and editing. KeP: Writing-original draft, Writing-review and editing. RP: Writing-original draft, Writing-review and editing. CP: Writing-original draft, Writing-review and editing. JP: Writing-original draft, Writing-review and editing. GP: Writing-original draft, Writing-review and editing. KaP: Writing-original draft, Writing-review and editing. PP: Writing-original draft, Writing-review and editing. SP: Writing-original draft, Writing-review and editing. AR: Writing-original draft, Writing-review and editing. SR: Writing-original draft, Writing-review and editing. AS: Writing-original draft, Writing-review and editing. DS_p: Writing-original draft, Writing-review and editing. JT: Writing-original draft, Writing-review and editing. NT-A: Writing-original draft, Writing-review and editing. DoW: Writing-original draft, Writing-review and editing. DaW: Writing-original draft, Writing-review and editing. JW: Writing-original draft, Writing-review and editing. WZ: Writing-original draft, Writing-review and editing. XZ: Writing-original draft, Writing-review and editing.

Funding

The author(s) declare that financial support was received for the research, authorship, and/or publication of this article. CP acknowledges funds by European Union - Next-Generation EU. JG and JP acknowledge support from NASA grants 80NSSC21K1567 and 80NSSC22K1120.

Acknowledgments

The work of DSt was carried out at the Jet Propulsion Laboratory, California Institute of Technology, under a contract with NASA. We thank the SIXTE support team for their assistance in generating spectra from simulated event files and for assistance with the documentation. We also thank Richard Barkus for his invaluable help with the art work and editing of the figures included in this paper.

Conflict of interest

The authors declare that the research was conducted in the absence of any commercial or financial relationships that could be construed as a potential conflict of interest.

Publisher's note

All claims expressed in this article are solely those of the authors and do not necessarily represent those of their affiliated organizations, or those of the publisher, the editors and the reviewers. Any product that may be evaluated in this article, or claim that may be made by its manufacturer, is not guaranteed or endorsed by the publisher.

References

Abbott, B. P., Abbott, R., Abbott, T. D., Acernese, F., Ackley, K., Adams, C., et al. (2017). Gravitational waves and gamma-rays from a binary neutron star merger: GW170817 and GRB 170817A. *ApJL* 848, L13. doi:10.3847/2041-8213/aa920c

Alford, J. A. J., Younes, G. A., Wadiasingh, Z., Abdelmaguid, M., An, H., Bachetti, M., et al. (2024). The high energy X-ray probe (HEX-P): magnetars and other isolated neutron stars. *Front. Astronomy Space Sci.* 10, 1294449. doi:10.3389/fspas.2023.1294449

Ananna, T. T., Treister, E., Urry, C. M., Ricci, C., Kirkpatrick, A., LaMassa, S., et al. (2019). The accretion history of AGNs. I. Supermassive black hole population synthesis model. *ApJ* 871, 240. doi:10.3847/1538-4357/aafb77

Ananna, T. T., Weigel, A. K., Trakhtenbrot, B., Koss, M. J., Urry, C. M., Ricci, C., et al. (2022). BASS. XXX. Distribution functions of DR2 Eddington ratios, black hole masses, and X-ray luminosities. *ApJS* 261, 9. doi:10.3847/1538-4365/ac5b64

Bachetti, M., Harrison, F. A., Walton, D. J., Grefenstette, B. W., Chakrabarty, D., Fürst, F., et al. (2014). An ultraluminous X-ray source powered by an accreting neutron star. *Nature* 514, 202–204. doi:10.1038/nature13791

Bachetti, M., Middleton, M. J., Pinto, C., Gúrpide, A., Walton, D. J., Brightman, M., et al. (2023). The high energy X-ray probe (HEX-P): studying extreme accretion with ultraluminous X-ray sources. *Front. Astronomy Space Sci.* 10, 1289432. doi:10.3389/fspas.2023.1289432

Baloković, M., Cabral, S. E., Brenneman, L., and Urry, C. M. (2021). Properties of the obscuring torus in NGC 1052 from multiepoch broadband X-ray spectroscopy. *ApJ* 916, 90. doi:10.3847/1538-4357/abf4d

Beckmann, R. S., Smethurst, R. J., Simmons, B. D., Coil, A., Dubois, Y., Garland, I. L., et al. (2024). Supermassive black holes in merger-free galaxies have higher spins which are preferentially aligned with their host galaxy. *MNRAS* 527, 10867–10877. doi:10.1093/mnras/stad1795

Berti, E., and Volonteri, M. (2008). Cosmological black hole spin evolution by mergers and accretion. *ApJ* 684, 822–828. doi:10.1086/590379

Blecha, L., Snyder, G. F., Satyapal, S., and Ellison, S. L. (2018). The power of infrared AGN selection in mergers: a theoretical study. *MNRAS* 478, 3056–3071. doi:10.1093/mnras/sty1274

Boorman, P. G., Torres-Albà, N., Annuar, A., Marchesi, S., Pfeifle, R., Stern, D., et al. (2023). The high energy X-ray probe (HEX-P): the circum-nuclear environment of growing supermassive black holes. doi:10.4550/arXiv.2311.04949

Bottacini, E., Ajello, M., and Greiner, J. (2012). The deep look at the hard X-ray sky: the swift-INTEGRAL X-ray (SIX) survey. *ApJS* 201, 34. doi:10.1088/0067-0049/201/2/34

Brightman, M., Margutti, R., Polzin, A., Jaodand, A., Hotokezaka, K., Alford, J. A. J., et al. (2024). The high energy X-ray probe (HEX-P): sensitive broadband X-ray observations of transient phenomena in the 2030s. *Front. Astronomy Space Sci.* 10, 1292656. doi:10.3389/fspas.2023.1292656

Buchner, J., Brightman, M., Baloković, M., Wada, K., Bauer, F. E., and Nandra, K. (2021). Physically motivated X-ray obscurer models. *Astron. Astrophys.* 651, A58. doi:10.1051/0004-6361/201834963

Buchner, J., Georgakakis, A., Nandra, K., Hsu, L., Rangel, C., Brightman, M., et al. (2014). X-ray spectral modelling of the AGN obscuring region in the CDFS: Bayesian model selection and catalogue. *Astron. Astrophys.* 564, A125. doi:10.1051/0004-6361/201322971

Burgess, D. A., Mori, K., Gelfand, J. D., Hailey, C. J., Tokayer, Y. M., Woo, J., et al. (2022). The eel pulsar wind nebula: a PeVatron-candidate origin for HAWC J1826–128 and HESS J1826–130. *ApJ* 930, 148. doi:10.3847/1538-4357/ac650a

Burns, E. (2020). Neutron star mergers and how to study them. *Living Rev. Relativ.* 23, 4. doi:10.1007/s41114-020-00028-7

Bustamante, S., and Springel, V. (2019). Spin evolution and feedback of supermassive black holes in cosmological simulations. *MNRAS* 490, 4133–4153. doi:10.1093/mnras/stz2836

Civano, F., Zhao, X., Boorman, P. G., Marchesi, S., Ananna, T., Creech, S., et al. (2024). The high energy X-ray probe (HEX-P): bringing the cosmic X-ray background into focus. *Front. Astronomy Space Sci.* 11, 1340719. doi:10.3389/fspas.2024.1340719

Connors, R. M. T., Tomsick, J. A., Draghis, P., Coughenour, B., Shaw, A. W., García, J. A., et al. (2024). The High Energy X-ray Probe (HEX-P): probing accretion onto stellar mass black holes. *Front. Astronomy Space Sci.* 10, 1292682. doi:10.3389/fspas.2023.1292682

De Marco, B., Ponti, G., Cappi, M., Dadina, M., Uttley, P., Cackett, E. M., et al. (2013). Discovery of a relation between black hole mass and soft X-ray time lags in active galactic nuclei. *MNRAS* 431, 2441–2452. doi:10.1093/mnras/stt339

De Rosa, A., Vignali, C., Bogdanović, T., Capelo, P. R., Charisi, M., Dotti, M., et al. (2019). The quest for dual and binary supermassive black holes: a multi-messenger view. *NewAR* 86, 101525. doi:10.1016/j.newar.2020.101525

Doeleman, S., Agol, E., Backer, D., Baganoff, F., Bower, G. C., Broderick, A., et al. (2009). “Imaging an event horizon: submm-VLBI of a super massive black hole,” in *astro2010: the astronomy and astrophysics decadal survey*, 2010, 68. doi:10.48550/arXiv.0906.3899

Dotti, M., Colpi, M., Pallini, S., Perego, A., and Volonteri, M. (2013). On the orientation and magnitude of the black hole spin in galactic nuclei. *ApJ* 762, 68. doi:10.1088/0004-637X/762/2/68

Drout, M. R., Piro, A. L., Shappee, B. J., Kilpatrick, C. D., Simon, J. D., Contreras, C., et al. (2017). Light curves of the neutron star merger GW170817/SSS17a: implications for r-process nucleosynthesis. *Science* 358, 1570–1574. doi:10.1126/science.aao0049

Dubois, Y., Beckmann, R., Bournaud, F., Choi, H., Devriendt, J., Jackson, R., et al. (2021). Introducing the NEWHORIZON simulation: galaxy properties with resolved internal dynamics across cosmic time. *Astron. Astrophys.* 651, A109. doi:10.1051/0004-6361/202039429

Dubois, Y., Pichon, C., Welker, C., Le Borgne, D., Devriendt, J., Laigle, C., et al. (2014). Dancing in the dark: galactic properties trace spin swings along the cosmic web. *MNRAS* 444, 1453–1468. doi:10.1093/mnras/stu1227

Eraerds, T., Antonelli, V., Davis, C., Hall, D. J., Hetherington, O., Holland, A. D., et al. (2021). Enhanced simulations on the athena/wide field imager instrumental background. *J. Astronomical Telesc. Instrum. Syst.* 7, 034001. doi:10.1111/1.JATIS.7.3.034001

Fürst, F., Walton, D. J., Harrison, F. A., Stern, D., Barret, D., Brightman, M., et al. (2016). Discovery of coherent pulsations from the ultraluminous X-ray source NGC 7793 P13. *ApJL* 831, L14. doi:10.3847/2041-8205/831/2/L14

Gautam, A., Crocker, R. M., Ferrario, L., Ruiter, A. J., Ploeg, H., Gordon, C., et al. (2022). Millisecond pulsars from accretion-induced collapse as the origin of the Galactic Centre gamma-ray excess signal. *Nat. Astron.* 6, 703–707. doi:10.1038/s41550-022-01658-3

Gilli, R., Comastri, A., and Hasinger, G. (2007). The synthesis of the cosmic X-ray background in the Chandra and XMM-Newton era. *A&A* 463, 79–96. doi:10.1051/0004-6361:20066334

Gravity+ Collaboration, Abuter, R., Alarcon, P., Allouche, F., Amorim, A., Baile, C., Bedigan, H., et al. (2022). The GRAVITY+ project: towards all-sky, faint-science, high-contrast near-infrared interferometry at the VLTI. *Messenger* 189, 17–22. doi:10.18727/0722-6691/5285

Grefenstette, B. W., Brightman, M., Earnshaw, H. P., Harrison, F. A., and Margutti, R. (2023). Early hard X-rays from the nearby core-collapse supernova SN 2023ixf. *ApJL* 952, L3. doi:10.3847/2041-8213/acdf4e

Griffin, A. J., Lacey, C. G., Gonzalez-Perez, V., Lagos, C. d. P., Baugh, C. M., and Fanidakis, N. (2019). The evolution of SMBH spin and AGN luminosities for $z < 6$ within a semi-analytic model of galaxy formation. *MNRAS* 487, 198–227. doi:10.1093/mnras/stz1216

Gúrpide, A., Parra, M., Godet, O., Contini, T., and Olive, J. F. (2022). MUSE spectroscopy of the ULX NGC 1313 X-1: a shock-ionised bubble, an X-ray photoionised nebula, and two supernova remnants. *A&A* 666, A100. doi:10.1051/0004-6361/202142229

Harding, A. K. (1996). Inverse-compton gamma-rays from plerions. *Space Sci. Rev.* 75, 257–268. doi:10.1007/BF00195038

Harrison, F. A., Aird, J., Civano, F., Lansbury, G., Mullaney, J. R., Ballantyne, D. R., et al. (2016). The NuSTAR extragalactic surveys: the number counts of active galactic nuclei and the resolved fraction of the cosmic X-ray background. *ApJ* 831, 185. doi:10.3847/0004-637X/831/2/185

Harrison, F. A., Craig, W. W., Christensen, F. E., Hailey, C. J., Zhang, W. W., Boggs, S. E., et al. (2013). The nuclear spectroscopic telescope Array (NuSTAR) high-energy X-ray mission. *ApJ* 770, 103. doi:10.1088/0004-637X/770/2/103

Hofmann, W., and Zanin, R. (2023). The Cherenkov telescope Array. 1, 47. doi:10.1007/978-981-16-4544-0_70-1

Hong, J., Mori, K., Hailey, C. J., Nynka, M., Zhang, S., Gotthelf, E., et al. (2016). NuSTAR hard X-ray survey of the galactic center region. II. X-ray point sources. *ApJ* 825, 132. doi:10.3847/0004-637X/825/2/132

IceCube Collaboration (2005). The IceCube neutrino telescope. *Nucl. Phys. B Proc. Suppl.* 138, 179–182. doi:10.1016/j.nuclphysbps.2004.11.042

Israel, G. L., Belfiore, A., Stella, L., Esposito, P., Casella, P., De Luca, A., et al. (2017). An accreting pulsar with extreme properties drives an ultraluminous x-ray source in NGC 5907. *Science* 355, 817–819. doi:10.1126/science.aai8635

Izquierdo-Villalba, D., Bonoli, S., Dotti, M., Sesana, A., Rosas-Guevara, Y., and Spinosa, D. (2020). From galactic nuclei to the halo outskirts: tracing supermassive black holes across cosmic history and environments. *MNRAS* 495, 4681–4706. doi:10.1093/mnras/staa1399

Jansen, F., Lumb, D., Altieri, B., Clavel, J., Ehle, M., Erd, C., et al. (2001). XMM-Newton observatory. I. The spacecraft and operations. *A&A* 365, L1–L6. doi:10.1051/0004-6361:20000036

Kammoun, E., Lohfink, A. M., Masterson, M., Wilkins, D. R., Zhao, X., Balokovic, M., et al. (2024). The high energy X-ray probe (HEX-P): probing the physics of

the X-ray corona in active galactic nuclei. *Front. Astronomy Space Sci.* 10, 1308056. doi:10.3389/fspas.2023.1308056

Kammoun, E. S., Miller, J. M., Koss, M., Oh, K., Zoghbi, A., Mushotzky, R. F., et al. (2020). A hard look at local, optically selected, obscured Seyfert galaxies. *ApJ* 901, 161. doi:10.3847/1538-4357/abb29f

Klein, O., and Nishina, T. (1929). Über die Streuung von Strahlung durch freie Elektronen nach der neuen relativistischen Quantendynamik von Dirac. *Z. für Phys.* 52, 853–868. doi:10.1007/BF01366453

Koss, M., Trakhtenbrot, B., Ricci, C., Lamperti, I., Oh, K., Berney, S., et al. (2017). BAT AGN spectroscopic survey. I. Spectral measurements, derived quantities, and AGN demographics. *ApJ* 850, 74. doi:10.3847/1538-4357/aa8ec9

Koss, M. J., Blecha, L., Bernhard, P., Hung, C.-L., Lu, J. R., Trakhtenbrot, B., et al. (2018). A population of luminous accreting black holes with hidden mergers. *Nature* 563, 214–216. doi:10.1038/s41586-018-0652-7

Koss, M. J., Trakhtenbrot, B., Ricci, C., Bauer, F. E., Treister, E., Mushotzky, R., et al. (2022). BASS. XXI. The data release 2 overview. *ApJS* 261, 1. doi:10.3847/1538-4365/ac6c8f

Kreykenbohm, I., Coburn, W., Wilms, J., Kretschmar, P., Staubert, R., Heindl, W. A., et al. (2002). Confirmation of two cyclotron lines in Vela X-1. *A&A* 395, 129–140. doi:10.1051/0004-6361:20021181

Kulkarni, S. R., Harrison, F. A., Grefenstette, B. W., Earnshaw, H. P., Andreoni, I., Berg, D. A., et al. (2021). Science with the ultraviolet explorer (UVEX). doi:10.48550/arXiv.2111.15608

Lattimer, J. M. (2011). Neutron stars and the dense matter equation of state. *Ap&SS* 336, 67–74. doi:10.1007/s10509-010-0529-1

Lawrence, A. (1991). The relative frequency of broad-lined and narrow-lined active galactic nuclei: implications for unified schemes. *MNRAS* 252, 586–592. doi:10.1093/mnras/252.4.586

Lehmer, B. D., Garofali, K., Binder, B. A., Fornasini, F., Vulic, N., Zezas, A., et al. (2023). The high energy X-ray probe: resolved X-ray populations in extragalactic environments. *Front. Astronomy Space Sci.* 10, 1293918. doi:10.3389/fspas.2023.1293918

Ludlam, R. M., Cackett, E. M., García, J. A., Miller, J. M., Stevens, A. L., Fabian, A. C., et al. (2022). Radius constraints from reflection modeling of Cygnus X-2 with NuSTAR and NICER. *ApJ* 927, 112. doi:10.3847/1538-4357/ac5028

Ludlam, R. M., Malacaria, C., Sokolova-Lapa, E., Fuerst, F., Pradhan, P., Shaw, A. W., et al. (2023). The high energy X-ray probe (HEX-P): a new window into neutron star accretion. *Front. Astronomy Space Sci.* 10, 1292500. doi:10.3389/fspas.2023.1292500

Luo, B., Brandt, W. N., Xue, Y. Q., Lehmer, B., Alexander, D. M., Bauer, F. E., et al. (2017). The Chandra deep field-south survey: 7 Ms source catalogs. *ApJS* 228, 2. doi:10.3847/1538-4365/228/1/2

Madsen, K. K., García, J. A., Stern, D., Amini, R., Basso, S., Coutinho, D., et al. (2024). The high energy X-ray probe (HEX-P): instrument and mission profile. *Front. Astronomy Space Sci.* 11, 1357834. doi:10.3389/fspas.2024.1357834

Marchesi, S., Zhao, X., Torres-Albà, N., Ajello, M., Gaspari, M., Pizzetti, A., et al. (2022). Compton-thick AGN in the NuSTAR era. VIII. A joint NuSTAR-XMM-Newton monitoring of the changing-look Compton-thick AGN NGC 1358. *ApJ* 935, 114. doi:10.3847/1538-4357/ac80be

Marcotulli, L., Ajello, M., Böttcher, M., Coppi, P., Costamante, L., Di Gesu, L., et al. (2023). The High Energy X-ray Probe (HEX-P): the most powerful jets through the lens of a superb X-ray eye. doi:10.48550/arXiv.2311.04801

Margutti, R., and Chornock, R. (2021). First multimessenger observations of a neutron star merger. *ARA& 59*, 155–202. doi:10.1146/annurev-astro-112420-030742

Margutti, R., Metzger, B. D., Chornock, R., Vurm, I., Roth, N., Grefenstette, B. W., et al. (2019). An embedded X-ray source shines through the aspherical at 2018cow: revealing the inner workings of the most luminous fast-evolving optical transients. *ApJ* 872, 18. doi:10.3847/1538-4357/aafa01

Meidinger, N., Albrecht, S., Beitler, C., Bonholzer, M., Emberger, V., Frank, J., et al. (2020). “Development status of the wide field imager instrument for Athena,” in *Society of photo-optical instrumentation engineers (SPIE) conference series*. Vol. 11444. doi:10.1117/12.2560507114440T

Miller, M. C., Lamb, F. K., Dittmann, A. J., Bogdanov, S., Arzoumanian, Z., Gendreau, K. C., et al. (2019). PSR J030+0451 mass and radius from NICER data and implications for the properties of neutron star matter. *ApJL* 887, L24. doi:10.3847/2041-8213/ab50c5

Moe, M., Kratter, K. M., and Badenes, C. (2019). The close binary fraction of solar-type stars is strongly anticorrelated with metallicity. *ApJ* 875, 61. doi:10.3847/1538-4357/ab0d88

Mori, K., An, H., Burgess, D., Capasso, M., Dingus, B., Gelfand, J., et al. (2022). “NuSTAR broad-band X-ray observational campaign of energetic pulsar wind nebulae in synergy with VERITAS, HAWC and Fermi gamma-ray telescopes,” in *37th International Cosmic Ray Conference*, 963. doi:10.22323/1.395.0963963

Mori, K., Hailey, C. J., Schutt, T. Y. E., Mandel, S., Heuer, K., Grindlay, J. E., et al. (2021). The X-ray binary population in the galactic center revealed through multi-decade observations. *ApJ* 921, 148. doi:10.3847/1538-4357/ac1da5

Mori, K., Ponti, G., Bachetti, M., Bodaghee, A., Grindlay, J., Hong, J., et al. (2024). The high energy X-ray probe (HEX-P): resolving the nature of Sgr A* flares, compact object binaries and diffuse X-ray emission in the Galactic center and beyond. *Front. Astronomy Space Sci.* 10, 1292130. doi:10.3389/fspas.2023.1292130

Mori, K., Reynolds, S., An, H., Bamba, A., Krivonos, R., Tsuji, N., et al. (2023). The high energy X-ray probe (HEX-P): galactic PeVatrons, star clusters, superbubbles, microquasar jets, and gamma-ray binaries. *Front. Astronomy Space Sci.* 10, 1303197. doi:10.3389/fspas.2023.1303197

Mosquera, A. M., Kochanek, C. S., Chen, B., Dai, X., Blackburne, J. A., and Chartas, G. (2013). The structure of the X-ray and optical emitting regions of the lensed quasar Q 2237+0305. *ApJ* 769, 53. doi:10.1088/0004-637X/769/1/53

Murase, K., Toomey, M. W., Fang, K., Oikonomou, F., Kimura, S. S., Hotokezaka, K., et al. (2018). Double neutron star mergers and short gamma-ray bursts: long-lasting high-energy signatures and remnant dichotomy. *ApJ* 854, 60. doi:10.3847/1538-4357/aaa48a

Nandra, K., Barret, D., Barcons, X., Fabian, A., den Herder, J.-W., Luigi, P., et al. (2013). The hot and energetic universe: a white paper presenting the science theme motivating the Athena+ mission. doi:10.48550/arXiv.1306.2307

National Academies of Sciences, E. and Medicine (2023). *Pathways to discovery in astronomy and astrophysics for the 2020s*. Washington, DC: The National Academies Press. doi:10.17226/26141

Novikov, I. D., and Thorne, K. S. (1973). “Astrophysics of black holes,” in *Black holes (les astres occlusi)*, 343–450.

Oppenheimer, J. R., and Volkoff, G. M. (1939). On massive neutron cores. *Phys. Rev.* 55, 374–381. doi:10.1103/PhysRev.55.374

Parker, M. L., Matzeu, G. A., Matthews, J. H., Middleton, M. J., Dauser, T., Jiang, J., et al. (2022). The X-ray disc/wind degeneracy in AGN. *MNRAS* 513, 551–572. doi:10.1093/mnras/stac877

Perez, K., Hailey, C. J., Bauer, F. E., Krivonos, R. A., Mori, K., Baganoff, F. K., et al. (2015). Extended hard-X-ray emission in the inner few parsecs of the Galaxy. *Nature* 520, 646–649. doi:10.1038/nature14353

Perley, D. A., Mazzali, P. A., Yan, L., Cenko, S. B., Gezari, S., Taggart, K., et al. (2019). The fast, luminous ultraviolet transient AT2018cow: extreme supernova, or disruption of a star by an intermediate-mass black hole? *MNRAS* 484, 1031–1049. doi:10.1093/mnras/sty3420

Peterson, B. M. (2014). Measuring the masses of supermassive black holes. *Space Sci. Rev.* 183, 253–275. doi:10.1007/s11214-013-9987-4

Pfeifle, R. W., Boorman, P. G., Weaver, K. A., Buchner, J., Civano, F., Madsen, K., et al. (2023). The high energy X-ray probe (HEX-P): the future of hard X-ray dual AGN science. doi:10.48550/arXiv.2311.05154

Pinto, C., Middleton, M. J., and Fabian, A. C. (2016). Resolved atomic lines reveal outflows in two ultraluminous X-ray sources. *Nature* 533, 64–67. doi:10.1038/nature17417

Piotrowska, J. M., García, J. A., Walton, D. J., Beckmann, R. S., Stern, D., Ballantyne, D. R., et al. (2023). The high energy X-ray probe (HEX-P): constraining supermassive black hole growth with population spin measurements. doi:10.48550/arXiv.2311.04752

Pooley, D., Blackburne, J. A., Rappaport, S., and Schechter, P. L. (2007). X-ray and optical flux ratio anomalies in quadruply lensed quasars. I. Zooming in on quasar emission regions. *ApJ* 661, 19–29. doi:10.1086/512115

Raijmakers, G., Greif, S. K., Hebel, K., Hinderer, T., Nissanke, S., Schwenk, A., et al. (2021). Constraints on the dense matter equation of state and neutron star properties from NICER’s mass-radius estimate of PSR J0740+6620 and multimessenger observations. *ApJL* 918, L29. doi:10.3847/2041-8213/ac089a

Remillard, R. A., and McClintock, J. E. (2006). X-ray properties of black-hole binaries. *ARA& 44*, 49–92. doi:10.1146/annurev.astro.44.051905.092532

Reynolds, C. (2021). “Observational constraints on black hole spin,” in *43rd COSPAR Scientific Assembly*, 28 January – 4 February, 1412.43

Reynolds, S., An, H., Abdelmaguid, M., Alford, J., Fryer, C., Mori, K., et al. (2023). The High Energy X-ray Probe (HEX-P): supernova remnants, pulsar wind nebulae, and nuclear astrophysics. *Front. Astronomy Space Sci.* 10, 1321278. doi:10.3389/fspas.2023.1321278

Reynolds, S. P. (2016). Hard X-ray emission from pulsar-wind nebulae. *J. Plasma Phys.* 82, 635820501. doi:10.1017/S0022377816000751

Ricci, C., Ueda, Y., Koss, M. J., Trakhtenbrot, B., Bauer, F. E., and Gandhi, P. (2015). Compton-thick accretion in the local universe. *ApJL* 815, L13. doi:10.1088/2041-8205/815/1/L13

Secunda, A., Cen, R., Kimm, T., Götzberg, Y., and de Mink, S. E. (2020). Delayed photons from binary evolution help reionize the universe. *ApJ* 901, 72. doi:10.3847/1538-4357/abae0a

Sesana, A., Barausse, E., Dotti, M., and Rossi, E. M. (2014). Linking the spin evolution of massive black holes to galaxy kinematics. *ApJ* 794, 104. doi:10.1088/0004-637X/794/2/104

Staubert, R., Trümper, J., Kendziorra, E., Klochkov, D., Postnov, K., Kretschmar, P., et al. (2019). Cyclotron lines in highly magnetized neutron stars. *A&A* 622, A61. doi:10.1051/0004-6361/201834479

Sun, L., Ruiz, M., Shapiro, S. L., and Tsokaros, A. (2022). Jet launching from binary neutron star mergers: incorporating neutrino transport and magnetic fields. *Phys. Rev. D* 105, 104028. doi:10.1103/PhysRevD.105.104028

Tanaka, Y., and Lewin, W. H. G. (1995). "Black hole binaries," in *X-Ray binaries*, 126–174.

Thorne, K. S. (1974). Disk-accretion onto a black hole. II. Evolution of the hole. *ApJ* 191, 507–520. doi:10.1086/152991

Titarchuk, L., and Lyubarskij, Y. (1995). Power-law spectra as a result of comptonization of the soft radiation in a plasma cloud. *ApJ* 450, 876. doi:10.1086/176191

Tolman, R. C. (1939). Static solutions of einstein's field equations for spheres of fluid. *Phys. Rev.* 55, 364–373. doi:10.1103/PhysRev.55.364

Tombesi, F., Cappi, M., Reeves, J. N., Palumbo, G. G. C., Braito, V., and Dadina, M. (2011). Evidence for ultra-fast outflows in radio-quiet active galactic nuclei. II. Detailed photoionization modeling of Fe K-shell absorption lines. *ApJ* 742, 44. doi:10.1088/0004-637X/742/1/44

Tombesi, F., Cappi, M., Reeves, J. N., Palumbo, G. G. C., Yaqoob, T., Braito, V., et al. (2010). Evidence for ultra-fast outflows in radio-quiet AGNs: I. Detection and statistical incidence of Fe K-shell absorption lines. *A&A* 521, A57. doi:10.1051/0004-6361/200913440

Tomsick, J. A., Boggs, S. E., Zoglauer, A., Hartmann, D., Ajello, M., Burns, E., et al. (2023). The Compton spectrometer and imager. doi:10.48550/arXiv.2308.12362

Torres-Albà, N., Marchesi, S., Zhao, X., Ajello, M., Silver, R., Ananna, T. T., et al. (2021). Compton-thick AGN in the NuSTAR era VI: the observed compton-thick fraction in the local universe. *ApJ* 922, 252. doi:10.3847/1538-4357/ab1c73

Torres-Albà, N., Marchesi, S., Zhao, X., Cox, I., Pizzetti, A., Sengupta, D., et al. (2023). Hydrogen column density variability in a sample of local Compton-thin AGN. *A&A* 678, A154. doi:10.1051/0004-6361/202345947

Ueda, Y., Akiyama, M., Hasinger, G., Miyaji, T., and Watson, M. G. (2014). Toward the standard population synthesis model of the X-ray background: evolution of X-ray luminosity and absorption functions of active galactic nuclei including compton-thick populations. *ApJ* 786, 104. doi:10.1088/0004-637X/786/2/104

Uttley, P., Cackett, E. M., Fabian, A. C., Kara, E., and Wilkins, D. R. (2014). X-ray reverberation around accreting black holes. *A&A Rev.* 22, 72. doi:10.1007/s00159-014-0072-0

Vasudevan, R. V., Fabian, A. C., Reynolds, C. S., Aird, J., Dauser, T., and Gallo, L. C. (2016). A selection effect boosting the contribution from rapidly spinning black holes to the cosmic X-ray background. *MNRAS* 458, 2012–2023. doi:10.1093/mnras/stw363

Weisskopf, M. C., Soffitta, P., Baldini, L., Ramsey, B. D., O'Dell, S. L., Romani, R. W., et al. (2022). Imaging X-ray polarimetry explorer: prelaunch. *J. Astronomical Telesc. Instrum. Syst.* 8, 026002. doi:10.1117/1.JATIS.8.2.026002

Wilk, D. R., Lehmer, B. D., Hornschemeier, A. E., Yukita, M., Ptak, A., Zezas, A., et al. (2014). Spatially resolving a starburst galaxy at hard X-ray energies: NuSTAR, Chandra, and VLBA observations of NGC 253. *ApJ* 797, 79. doi:10.1088/0004-637X/797/2/79

Zhao, X., Civano, F., Fornasini, F. M., Alexander, D. M., Cappelluti, N., Chen, C. T., et al. (2021). The NuSTAR extragalactic survey of the james webb space telescope north ecliptic Pole time-domain field. *MNRAS* 508, 5176–5195. doi:10.1093/mnras/stab2885

Zhao, X., Civano, F., Willmer, C. N. A., Bonoli, S., Chen, C.-T., Creech, S., et al. (2024). PEARLS: NuSTAR and XMM-Newton extragalactic survey of the JWST north ecliptic Pole time-domain field II. *arXiv e-prints* 965, 188. doi:10.3847/1538-4357/ad2b61

Copyright © 2024 García, Stern, Madsen, Smith, Grefenstette, Ajello, Alford, Annuar, Bachetti, Baloković, Beckmann, Bianchi, Biccaro, Boorman, Brightman, Buchner, Bulbul, Chen, Civano, Coley, Connors, Del Santo, Gesu, Draghis, Fragile, Gürpide, Gangi, Gezari, Harrison, Kammoun, Lanzuisi, Lehmer, Lohfink, Ludlam, Marchesi, Marcotulli, Margutti, Masterson, Merloni, Middleton, Mori, Moretti, Nandra, Perez, Pfeifle, Pinto, Piotrowska, Ponti, Pottschmidt, Predehl, Puccetti, Rau, Reynolds, Santangelo, Spiga, Tomsick, Torres-Albà, Walton, Wilkins, Wilms, Zhang and Zhao. This is an open-access article distributed under the terms of the [Creative Commons Attribution License \(CC BY\)](https://creativecommons.org/licenses/by/4.0/). The use, distribution or reproduction in other forums is permitted, provided the original author(s) and the copyright owner(s) are credited and that the original publication in this journal is cited, in accordance with accepted academic practice. No use, distribution or reproduction is permitted which does not comply with these terms.